NASA TECHNICAL MEMORANDUM

NASA TM X-62,047

NASA TM X-62,047

WIND TUNNEL PRESSURE SIGNATURES FOR A .016–SCALE MODEL OF THE APOLLO COMMAND MODULE

Joel P. Mendoza and Raymond M. Hicks

Ames Research Center
Moffett Field, Calif. 94035

July 1971

WIND TUNNEL PRESSURE SIGNATURES FOR A .016-SCALE MODEL OF THE APOLLO COMMAND MODULE

By Joel P. Mendoza and Raymond M. Hicks
Ames Research Center

ABSTRACT

Pressure signatures were measured at roll angles ranging from 0° to 180° for a .016-scale model of the Apollo Command Module spacecraft at 25° angle of attack. The test Mach numbers ranged from 1.50 to 10.02.

WIND TUNNEL PRESSURE SIGNATURES FOR A .016-SCALE MODEL OF THE APOLLO COMMAND MODULE

By Joel P. Mendoza and Raymond M. Hicks
Ames Research Center

SUMMARY

A wind tunnel test was conducted to measure the overpressure characteristics of the .016-scale model of the Apollo command module. Pressure signatures for the model at 25° angle of attack were measured at roll angles ranging from 0° to 180°. Schlieren photographs were taken at 0° roll angle. The test Mach numbers ranged from 1.50 to 10.02.

INTRODUCTION

An investigation is underway to define the level of sonic-boom overpressure generated by space shuttle booster, orbiter and launch configurations during flight within the Earth's atmosphere. The procedure for determining sonic-boom overpressures on the ground is to define the near-field pressure signatures for the range of anticipated flight conditions and then to extrapolate these signatures to the far-field (ground). Near-field pressure signatures can be accurately measured in ground-based test facilities, but theory must be used to perform the extrapolations.

The Ames Sonic-Boom Extrapolation Technique described in reference 1 has been shown in references 2 and 3 to provide accurate results for widely different configurations at Mach numbers between 1.20 and 4.63. The accuracy of the technique was further illustrated in reference 4 by comparisons of extrapolated pressure signatures with those measured during overflights of the XB-70 and X-15 airplanes. However, the conditions for which the extrapolation technique has been verified differ from those expected for elements of the shuttle system. Shuttle operations include maneuvering flight at Mach numbers extending well into the hypersonic regime while verifications have been made only for steady unaccelerated flight conditions at Mach numbers less than 5. Therefore, consideration is being given to evaluation of the extrapolation technique using the Apollo command module as the test vehicle since some of its trajectory parameters are similar to those for the shuttle vehicles.

The purpose of this report is to present wind-tunnel measurements of near-field pressure signatures for a model of the Apollo command module. These pressure signatures can be used to obtain estimates of

ground-level overpressures produced by Apollo command modules re-entering the Earth's atmosphere.

NOTATION

d	model diameter (0.0635 meters)
h	altitude measured from the center-line of sting. (This line passes through the center of gravity of the full-scale Apollo command module)
M	Mach number
p	reference pressure
Δp	sonic boom overpressure
Δx	incremental longitudinal distance measured along the axis of the wind tunnel
α	angle of attack, degrees
ϕ	roll angle, degrees

MODEL AND TEST PROCEDURES

A .016-scale model of the Apollo command module was tested in the 20-inch (0.508-meter) supersonic and in the 21-inch (0.533-meter) hypersonic wind tunnels at the Jet Propulsion Laboratory. The model was set at 25° angle of attack for all of the test Mach numbers. A sketch of the model is shown in figure 1(a) and the model installed in the 20-inch supersonic wind tunnel at zero roll angle is shown in figure 1(b). For both the spacecraft and the model the roll axis is collinear with the velocity vector. The roll angle is specified as the angle between the pitch plane of the model and the vertical plane passing through the axis of the overpressure probe. At each Mach number pressure signatures were measured for roll angles between 0° and 180° in increments of 30°.

The pressure signatures were measured using a system consisting of an overpressure probe and a pressure transducer. The overpressure probe was a slender cone having an included angle of 2°. The probe had 4 pressure orifices, 90° apart, around the circumference of the circular cross section of the cone. The 4 pressure orifices were

manifolded together into a common chamber. The variation of the total-pressure throughout the test Mach number range is shown in the following table.

MACH NUMBER	TOTAL PRESSURE, mm-Hg
1.50	700
2.00	700
2.60	750
3.20	750
3.98	1000
5.98	1000
7.75	1500
10.02	8000

A remotely controlled linear actuator in the wind tunnel translated the model, relative to the fixed measuring equipment, longitudinally along a line parallel to the axis of the wind tunnel.

PRESENTATION OF THE DATA

Data in the form of Schlieren photographs and overpressure characteristics, for the .016-scale model of the Apollo command module at 25° angle of attack are presented in figures 2 through 12.

Schlieren photographs of model are shown at 0° roll angle in figure 2 for test Mach numbers ranging from 1.50 to 7.75. At Mach number 1.50 the bow shock wave is nearly symmetrical, the shock angle above and below the model appearing to be nearly equal. At the higher Mach numbers, the asymmetry of the shock becomes more distinct.

Shown in figure 3 for each Mach number are values of the maximum overpressure (shock strength) plotted against roll angle. The nearly symmetrical shock previously shown in figure 2 for the Mach number of 1.50 produces a relatively small variation of maximum overpressure with roll angle. Successively larger variations of the maximum

overpressure with roll angle occur with increasing Mach numbers. This also is consistent with the variations in bow shock wave geometry shown in figure 2. At Mach numbers 5.98 and 7.75 the maximum overpressure levels shown for the roll angles from 0° to 120° were measured at altitudes slightly different from those for the results at roll angle of 150° and 180°. These differences, are considered to be sufficiently small so that a curve connecting all of the data points would be representative of a constant altitude curve. Pressure signatures for the various roll angles are shown in figures 4 through 11 for all of the test Mach numbers. At the Mach number of 10.02 only one pressure signature was measured. At the Mach number of 7.75 the presence of a shock wave is noted in the expansion region of the pressure signatures measured with the model at the following roll angles: 0°, 30°, 60° and 90° (figures 10(a), 10(b)). This shock, also evidenced in the pressure signature measured at the Mach number of 10.02 (figure 11) is considered to be caused by sting interference. It is believed that the data can be corrected for these sting interference effects by extrapolating smooth curves faired through the data ahead of the shock waves. Results are presented in figure 12.

REFERENCES

1. Thomas, Charles L.: Extrapolation of Wind Tunnel Sonic Boom Signatures Without Use of the Whitham F-Function. NASA SP-255, 1971.

2. Hicks, Raymond M.; Mendoza, Joel P.; and Levy, Lionel L. Jr.: An Investigation of the Sonic Boom for Straight- and Delta-Wing Space Shuttle Orbiters. NASA TM X-62,030, April 9, 1969.

3. Mendoza, Joel P.; and Hicks, Raymond M.: On the Extrapolation of Measured Near-Field Pressure Signatures of Unconventional Configurations. NASA SP-255, 1971.

4. Hicks, Raymond M.; Mendoza, Joel P.; and Hunton, Lynn W.: Some Effects of Mach Number and Geometry on Sonic Boom. NASA TN D-4214, October 1967.

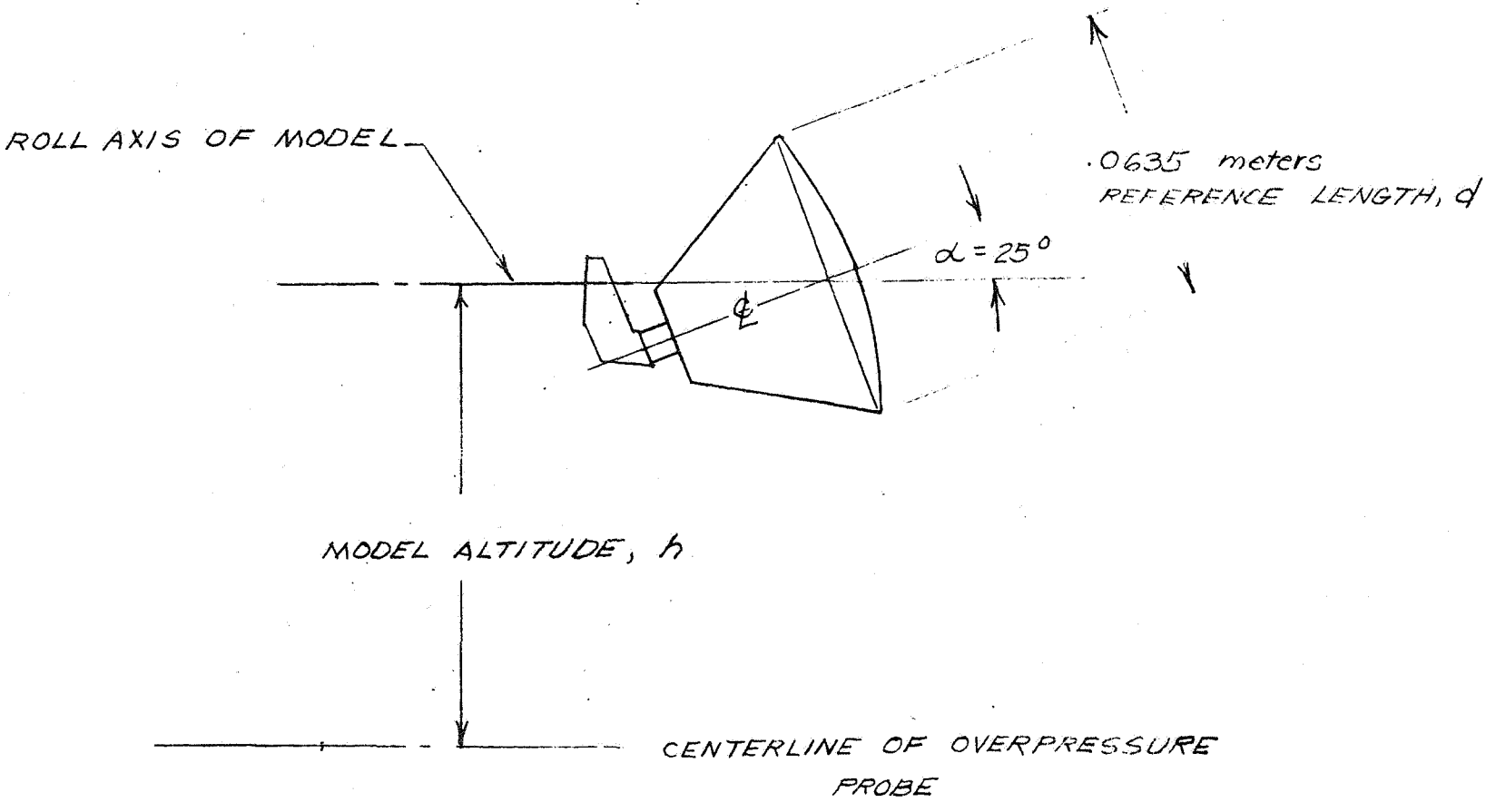

(a) SKETCH ILLUSTRATING NOMENCLATURE.

FIGURE 1. - .016 - SCALE MODEL OF THE APOLLO COMMAND MODULE. $\alpha = 25^{\circ}$, $\phi = 0.^{\circ}$

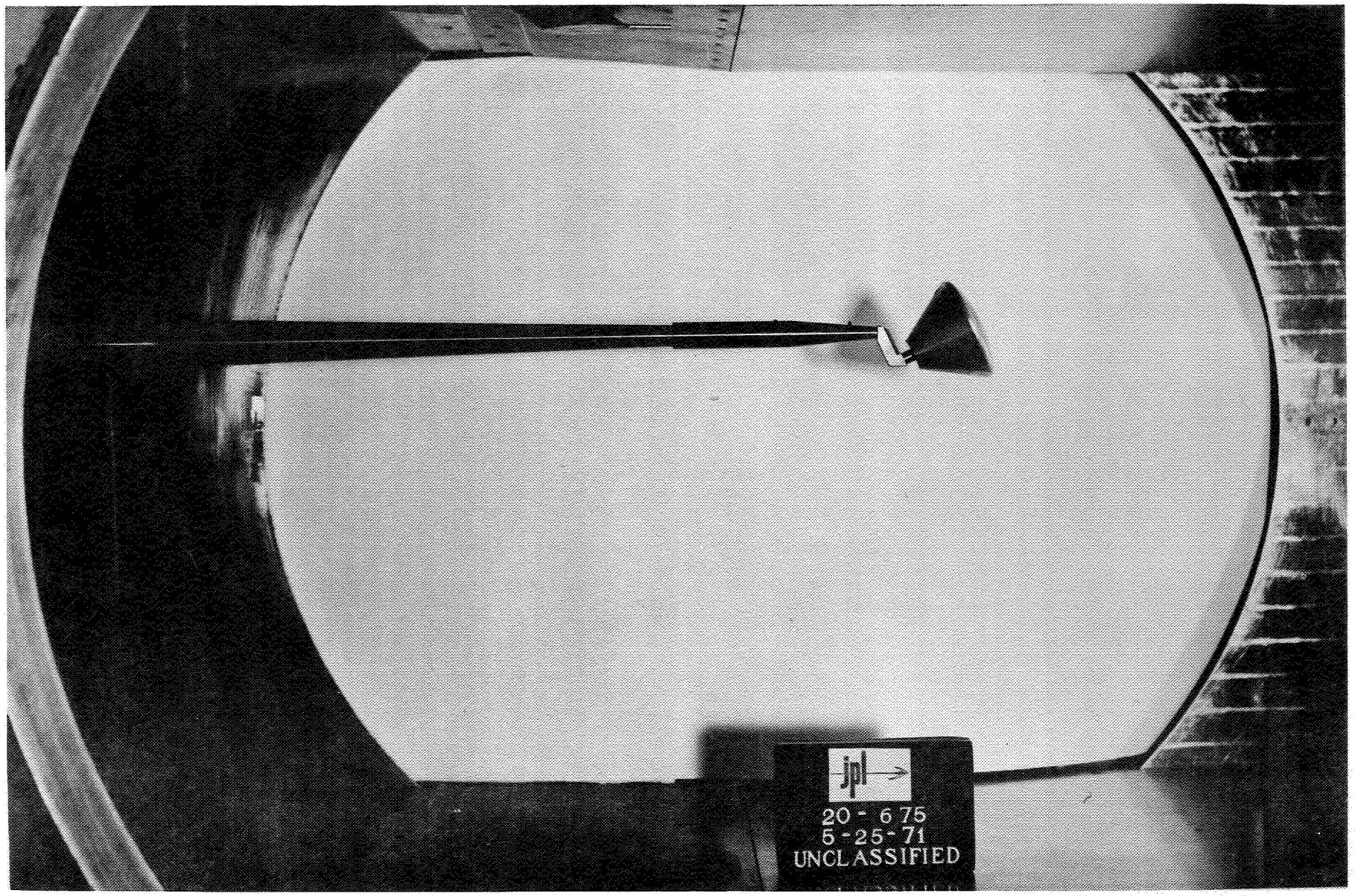

(b) Installation photograph showing model in 20-inch supersonic wind tunnel at the Jet Propulsion Laboratory.

Figure 1.- Concluded

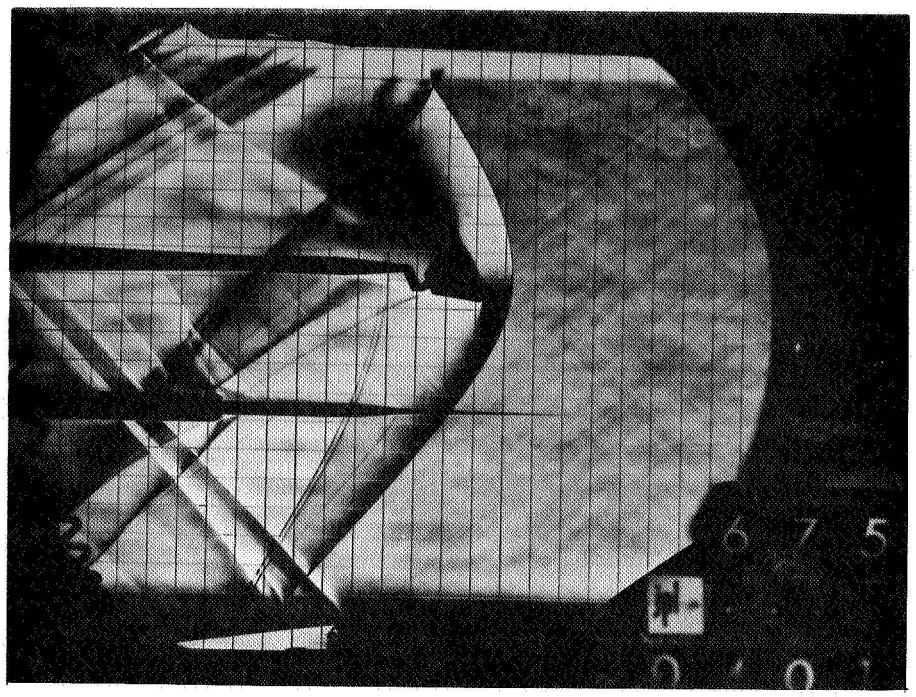

$M = 1.50$

$h/d = 2.05$

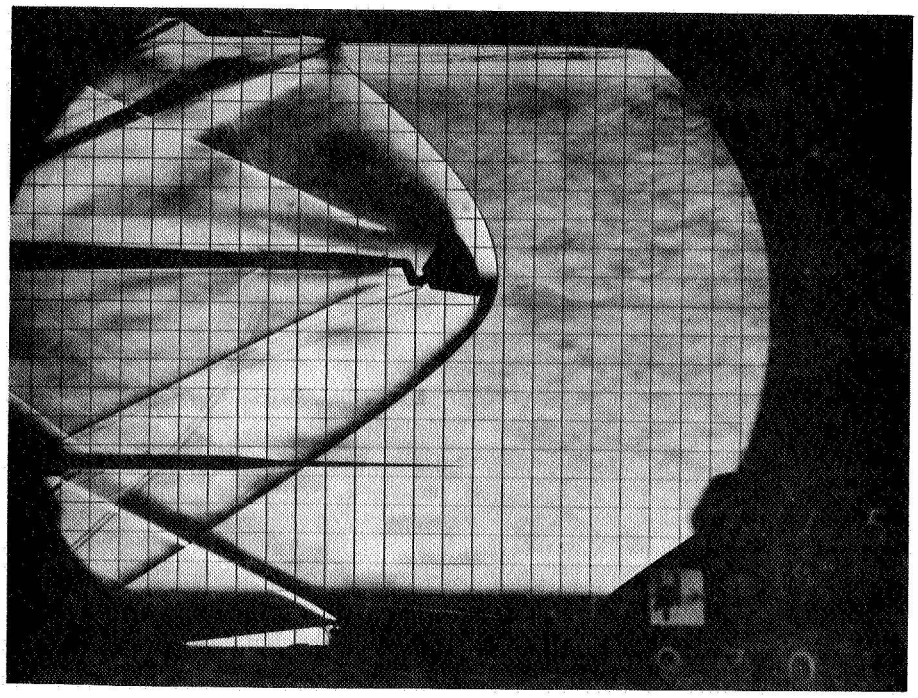

$M = 2.00$

$h/d = 2.85$

(a) $M = 1.50,\ 2.00;\ h/d = 2.85$

Figure 2.— Schlieren Photographs, $\phi = 0°$

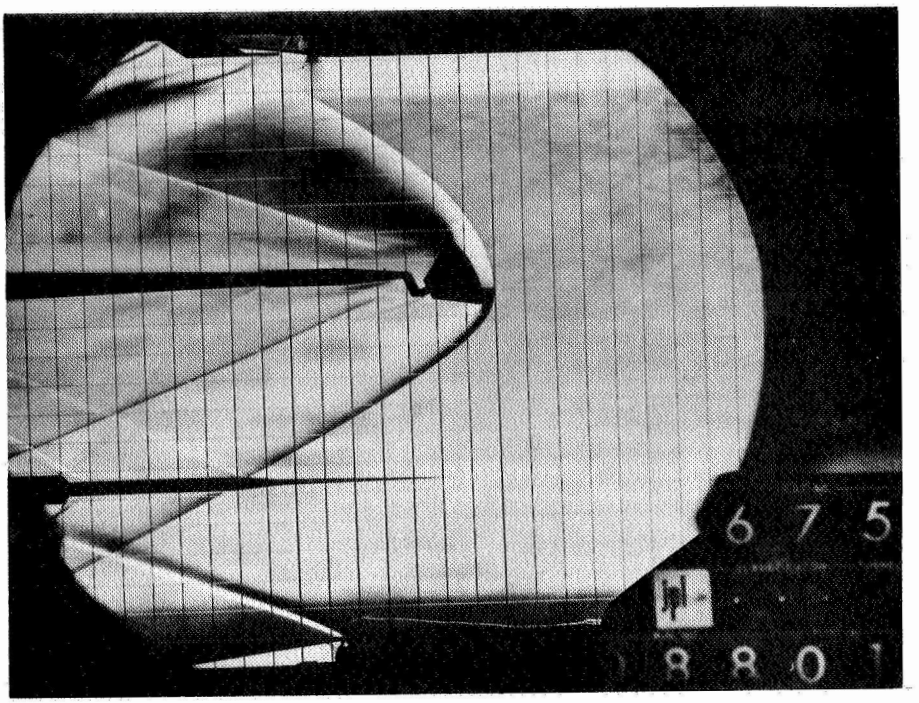

M = 2.60

h/d = 2.85

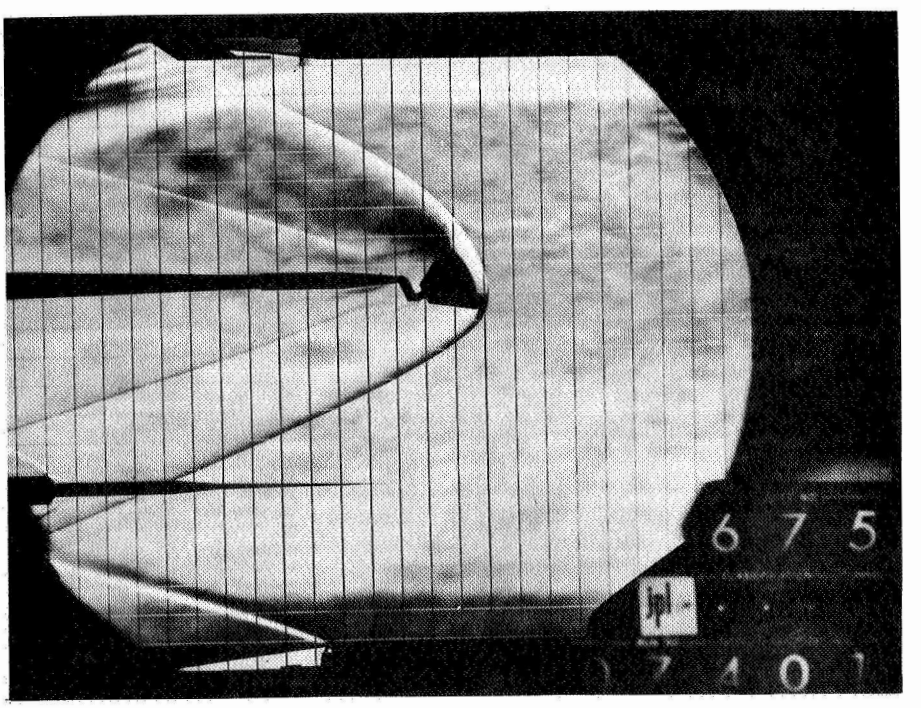

M = 3.20

h/d = 2.85

(b) M = 2.60, 3.20 ; h/d = 2.85

Figure 2.- Continued

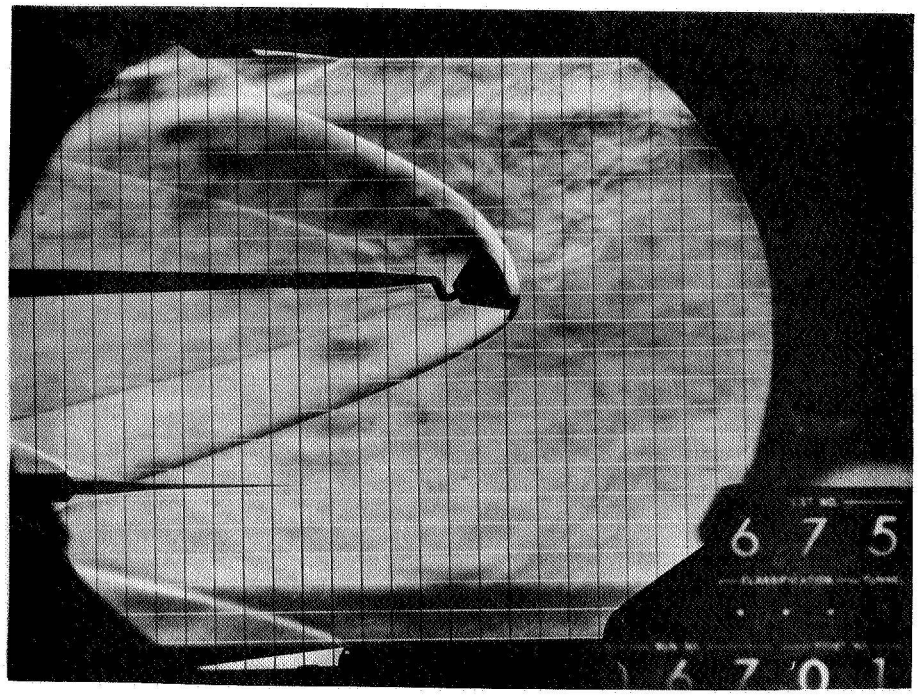

M = 3.98

h/d = 2.85

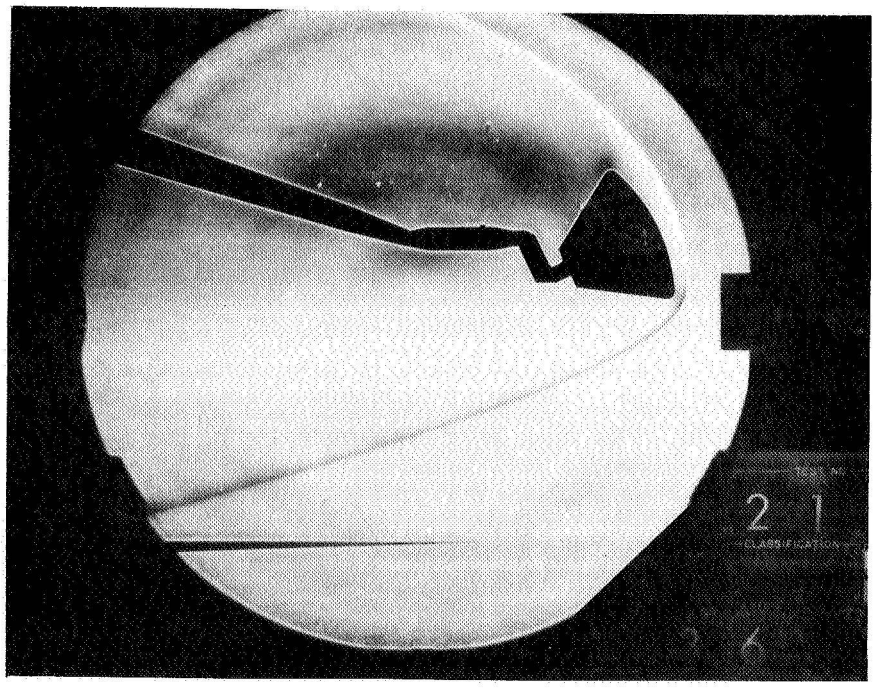

M = 5.98

h/d = 2.15

(c) M = 3.98, h/d = 2.85; M = 5.98, h/d = 2.15

Figure 2.- Continued

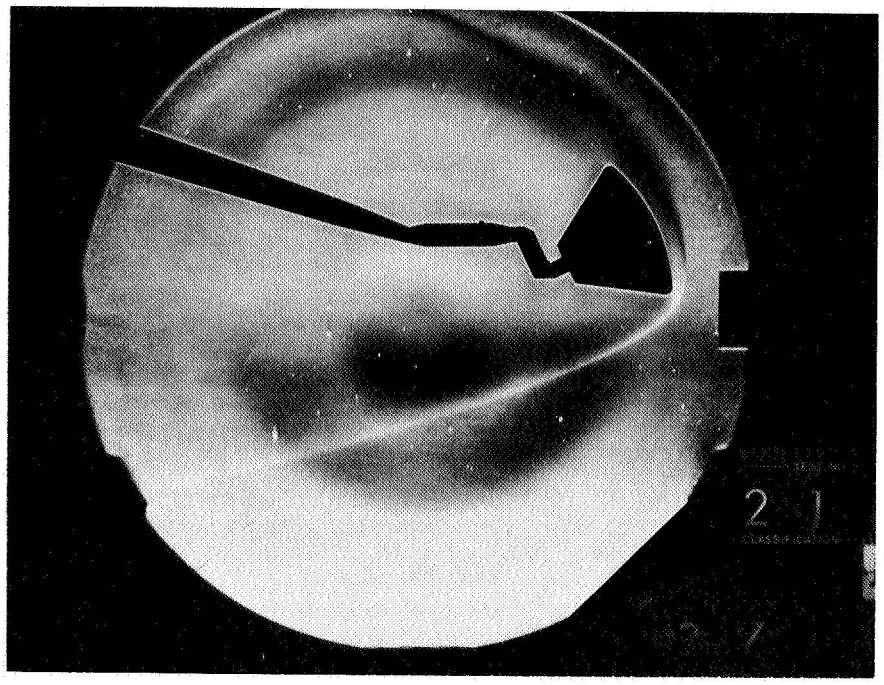

M = 7.75

h/d = 2.43

(d) M = 7.75, h/d = 2.43

Figure 2.- Concluded

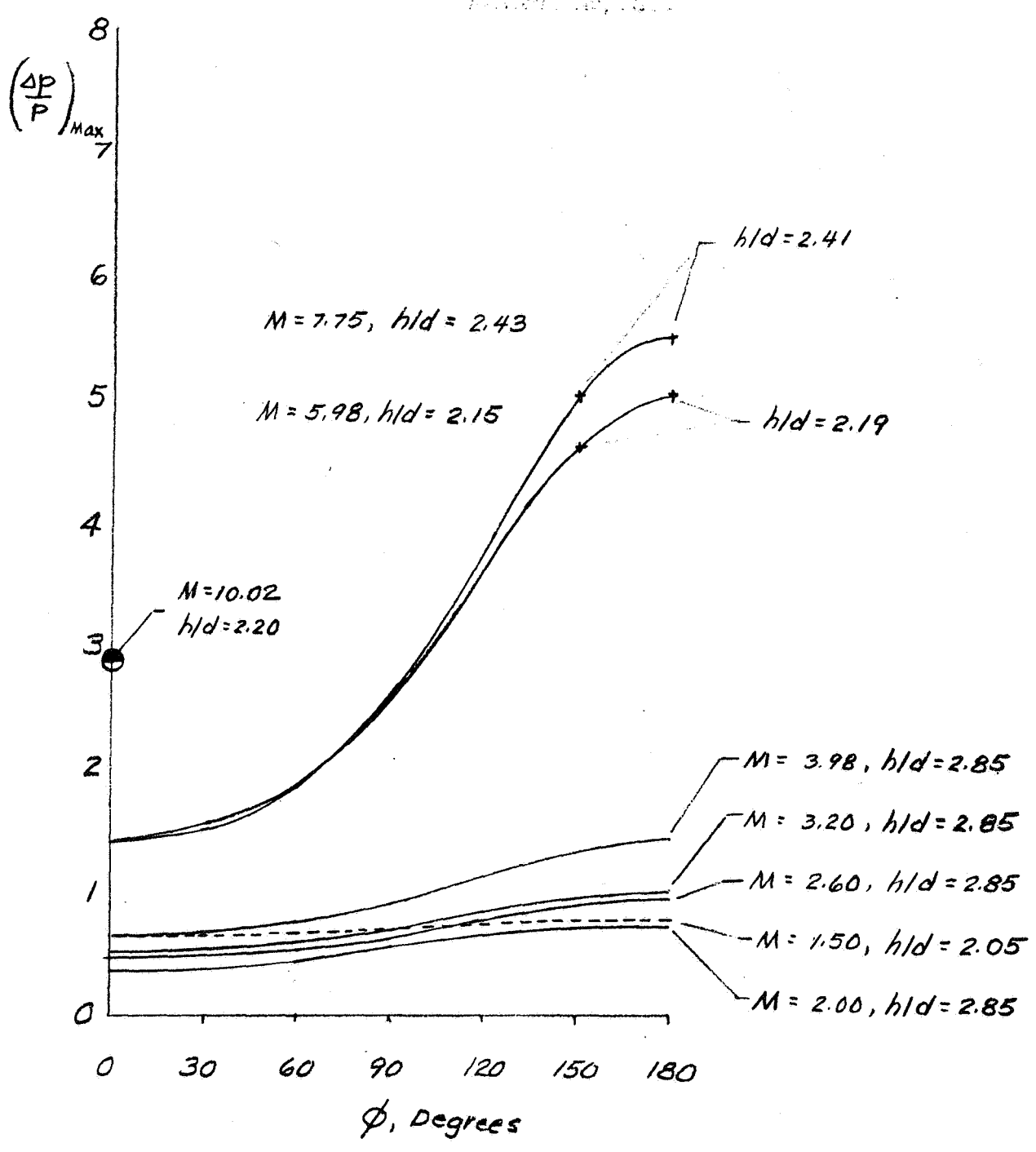

Figure 3.- Variation of the maximum overpressure with roll angle.

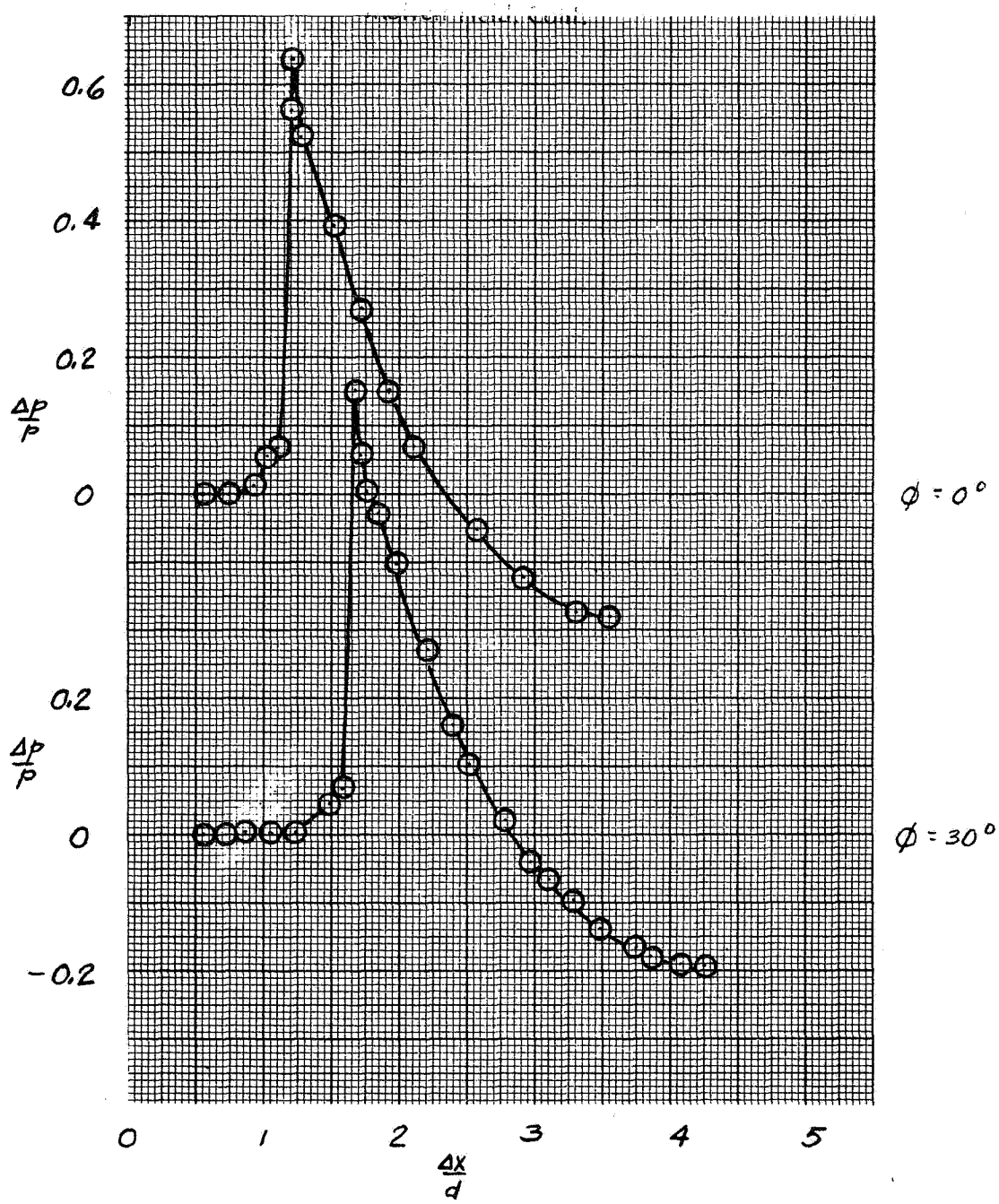

(a) $\phi = 0°, 30°$

Figure 4 - Pressure Signatures, $M = 1.5$, $\alpha = 25°$, $h/d = 2.05$

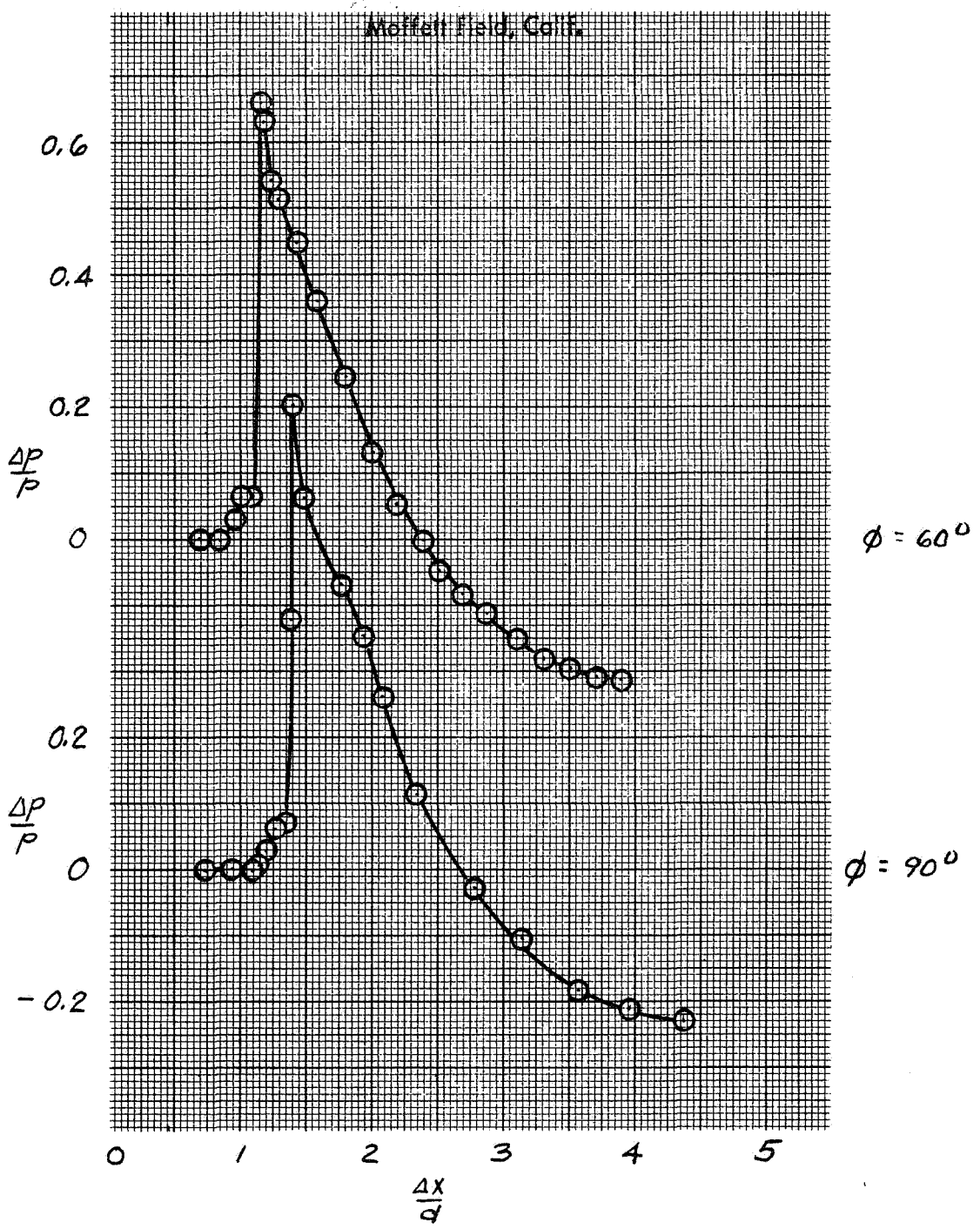

(b) $\phi = 60^\circ, 90^\circ$

Figure 4 - Continued

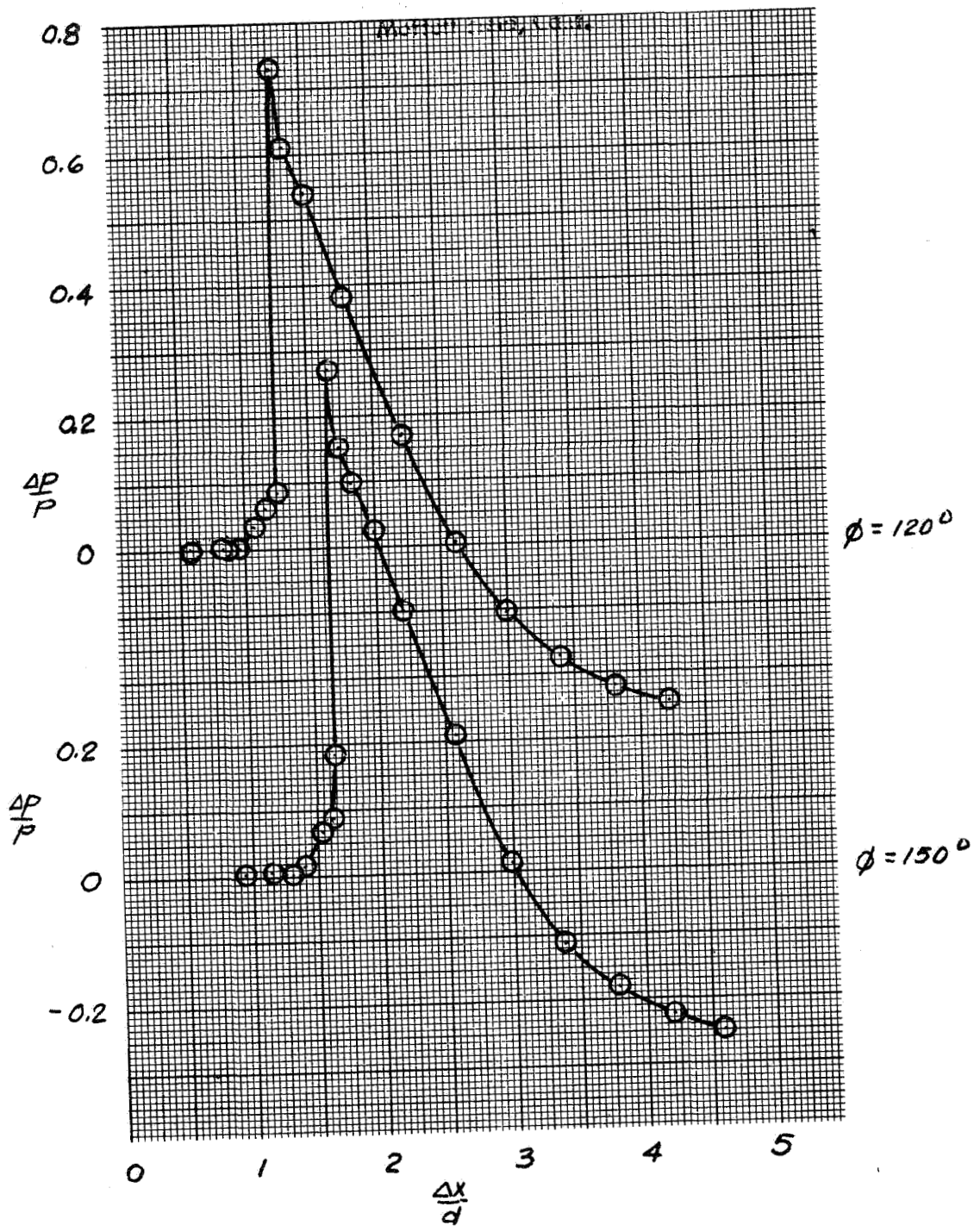

(c) $\phi = 120^\circ, 150^\circ$

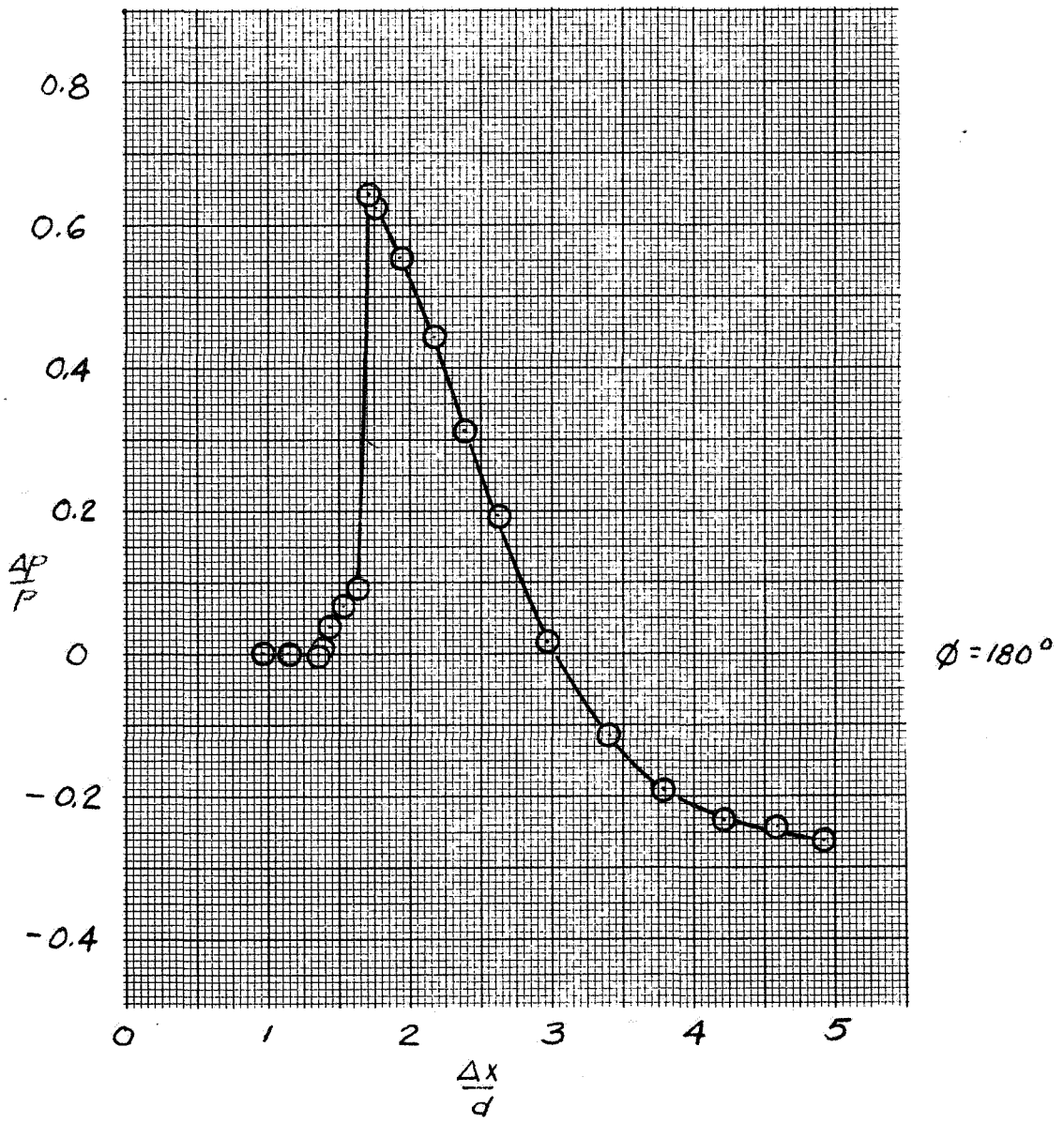

(d) $\phi = 180°$

Figure 4.- Concluded

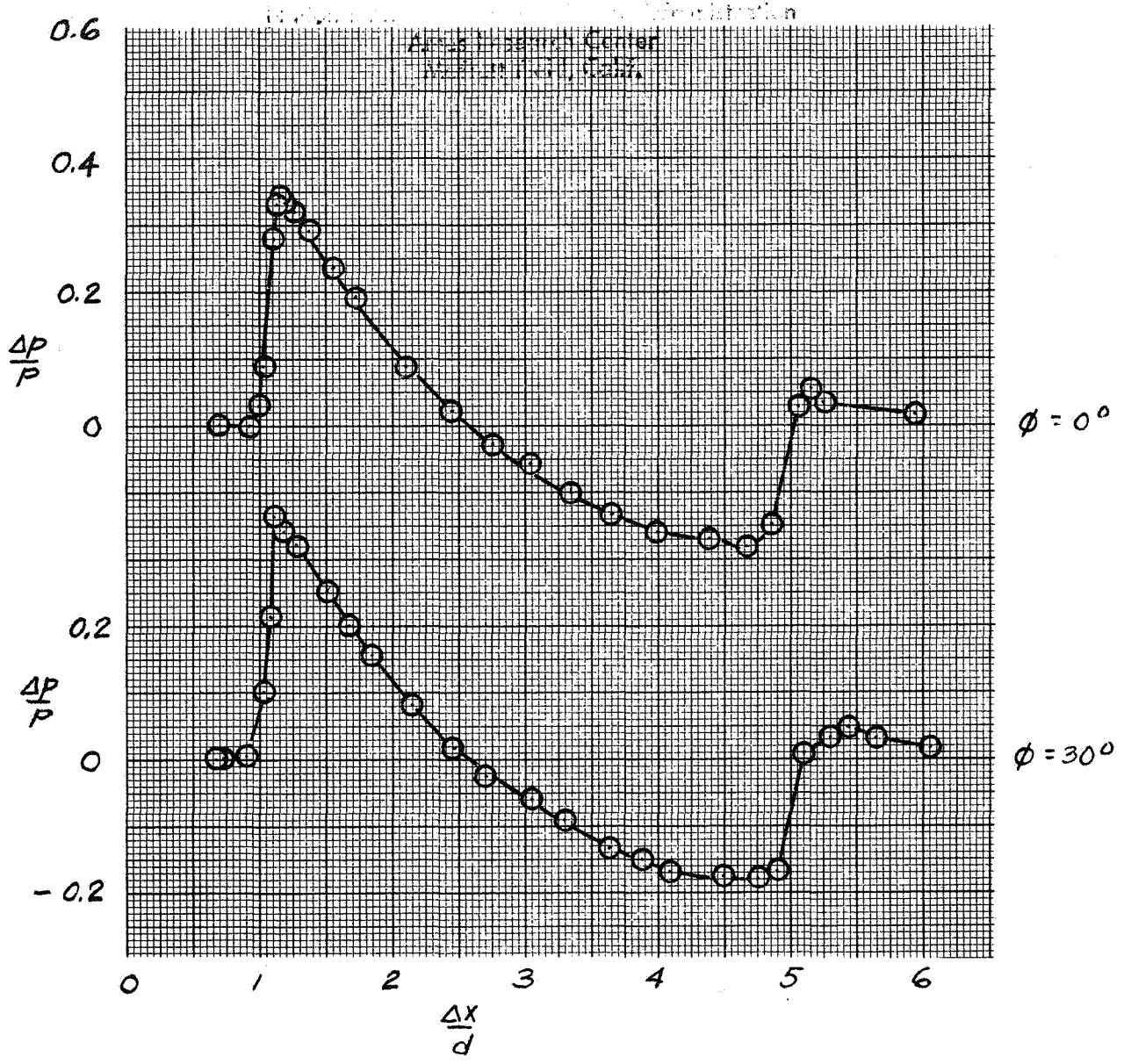

(a) $\phi = 0°, 30°$

Figure 5.- Pressure signatures, $M = 2.0$, $\alpha = 25°$, $h/d = 2.85$

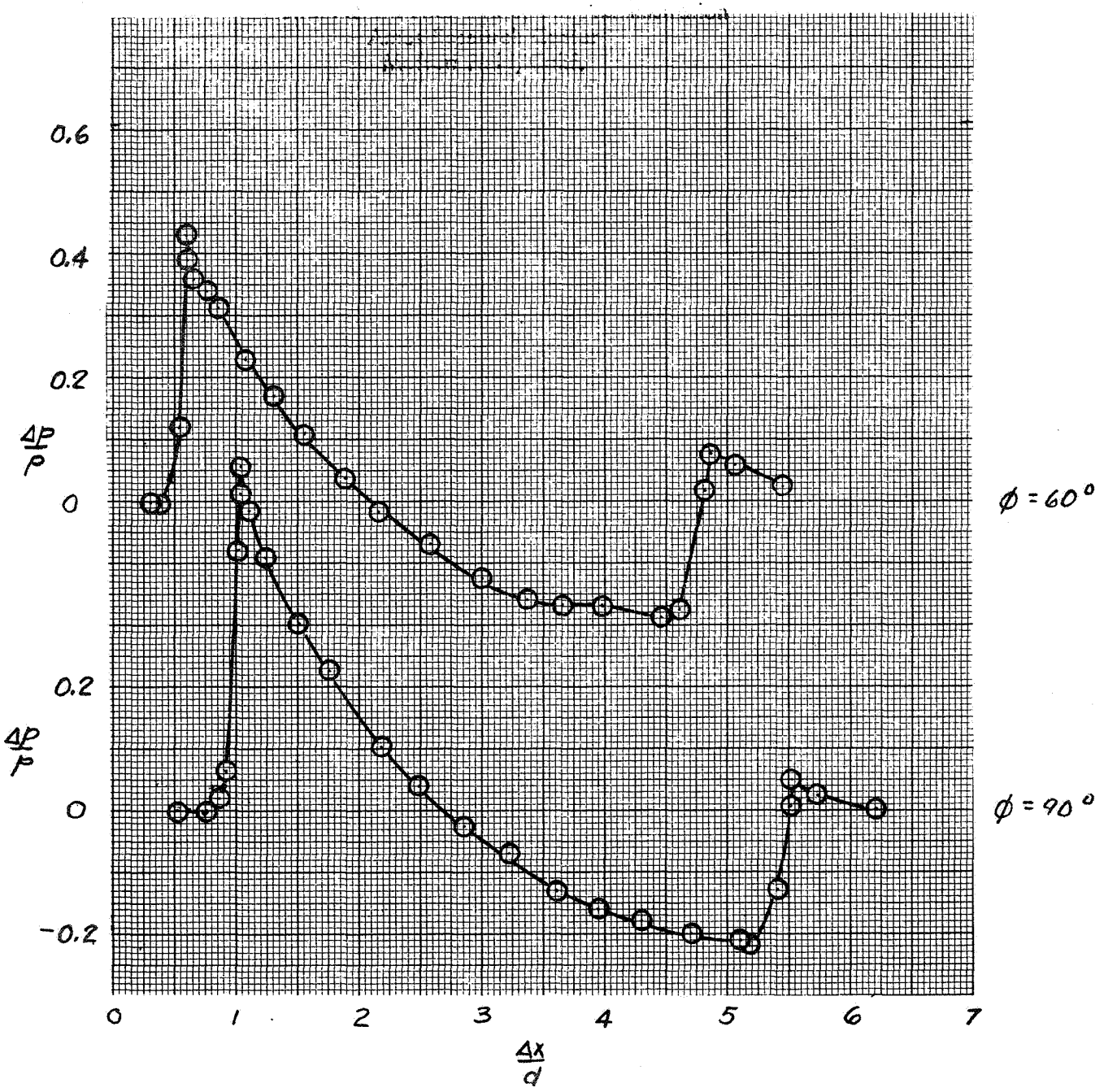

(b) $\phi = 60°, 90°$

Figure 5. - Continued

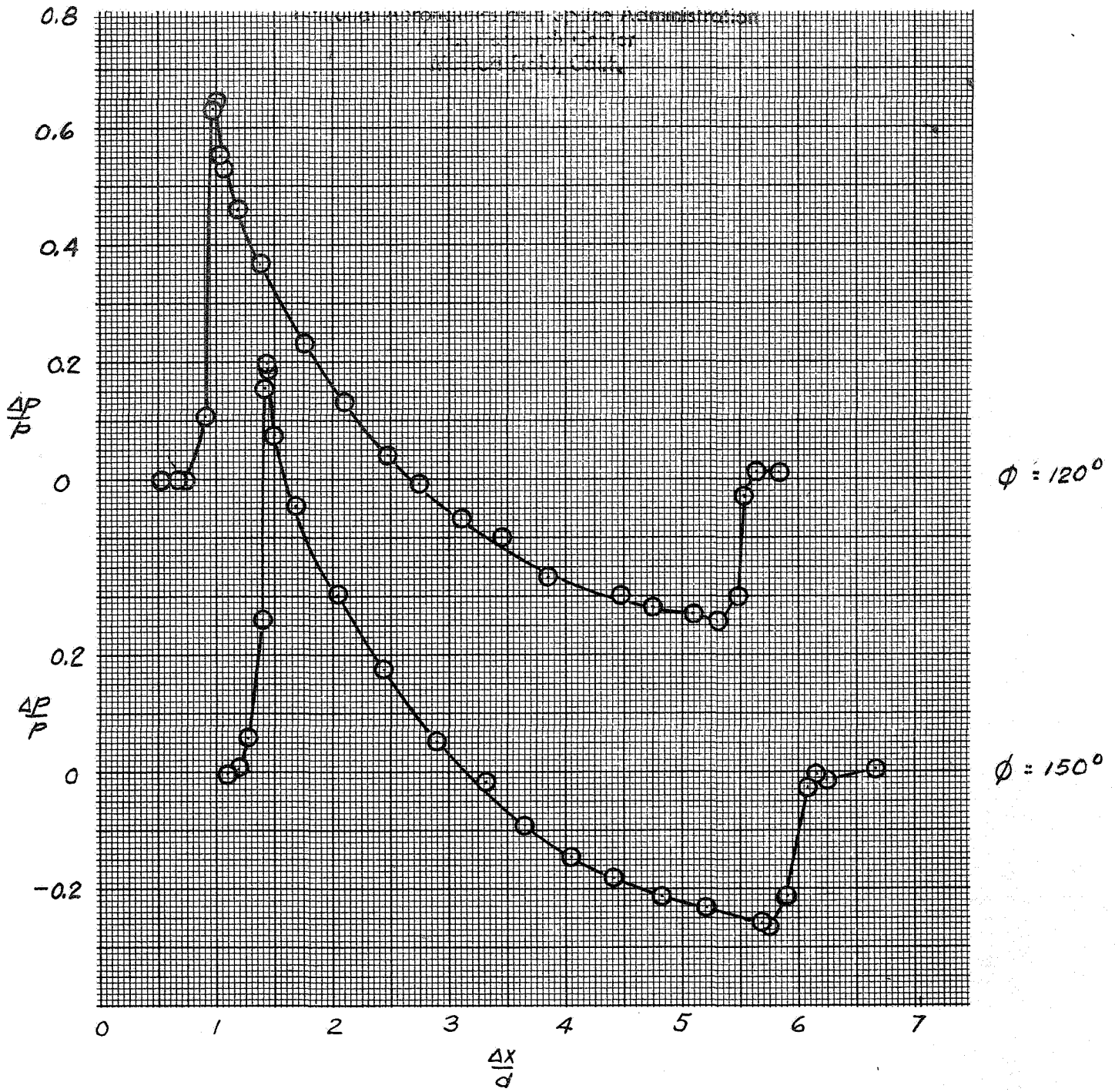

(c) $\phi = 120°, 150°$

Figure 5. - Continued

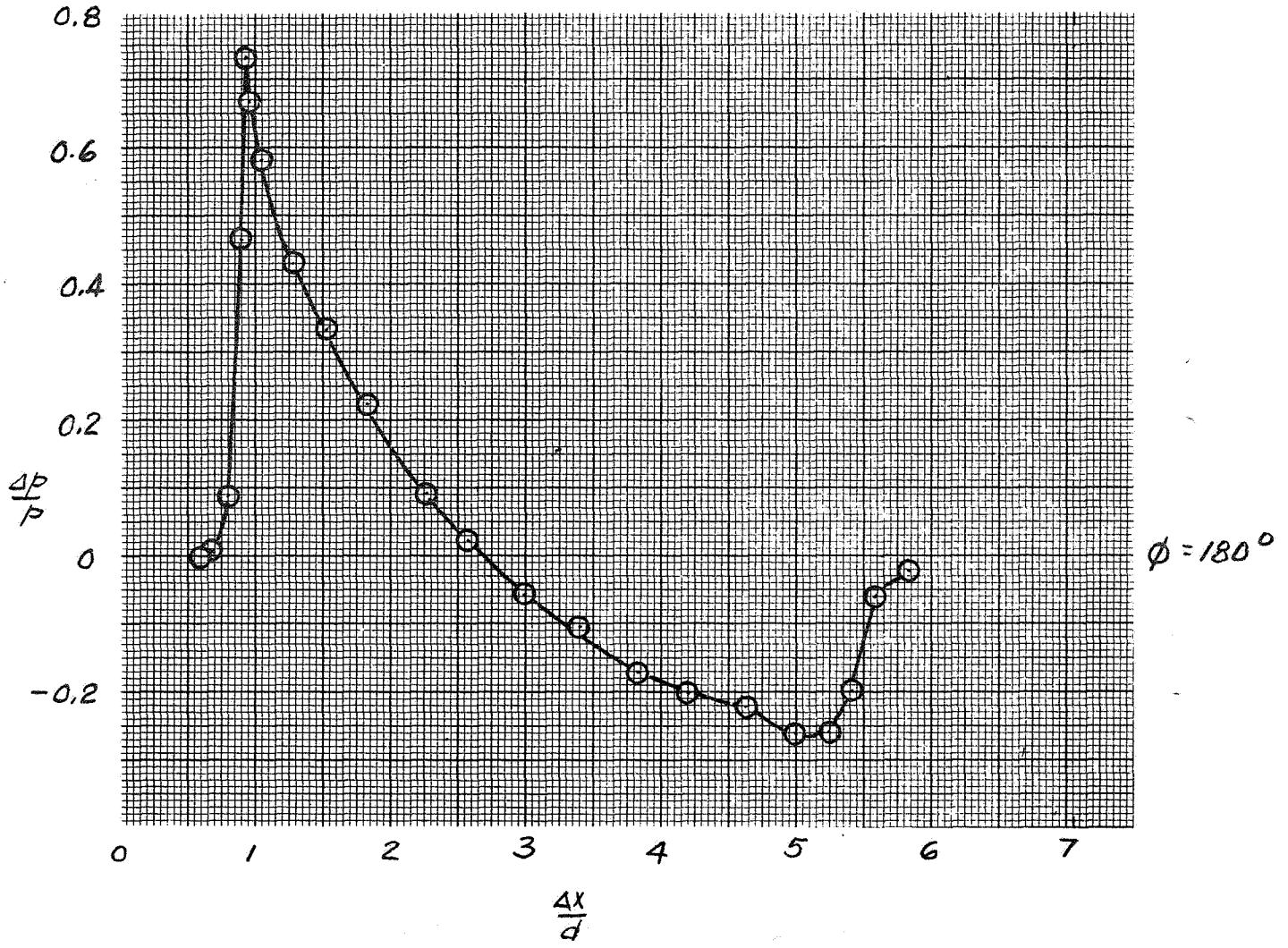

(d) $\phi = 180^\circ$

Figure 5.- Concluded

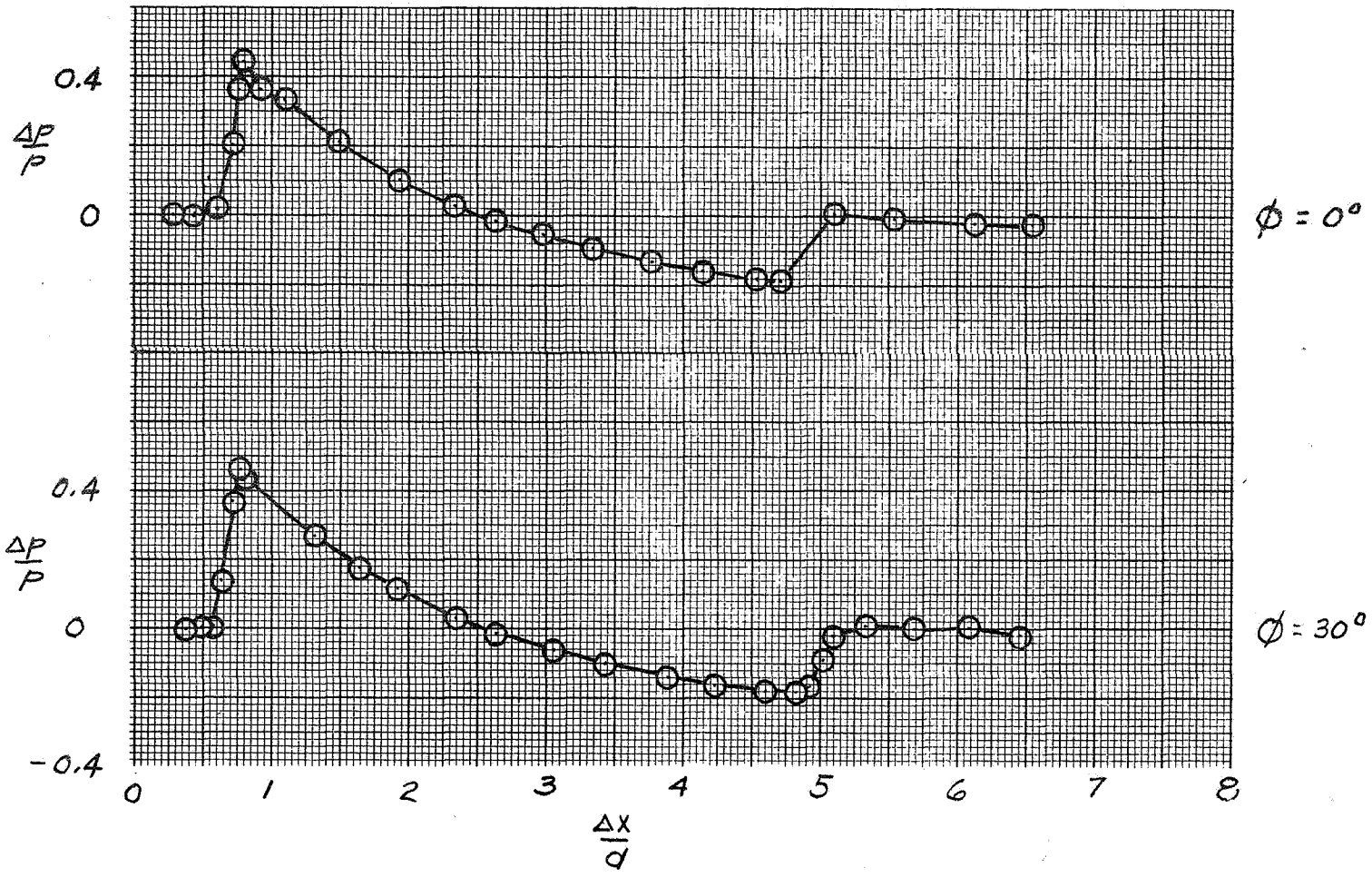

(a) $\phi = 0°, 30°$

Figure 6. - Pressure signatures, $M = 2.6$, $\alpha = 25°$, $h/d = 2.85$

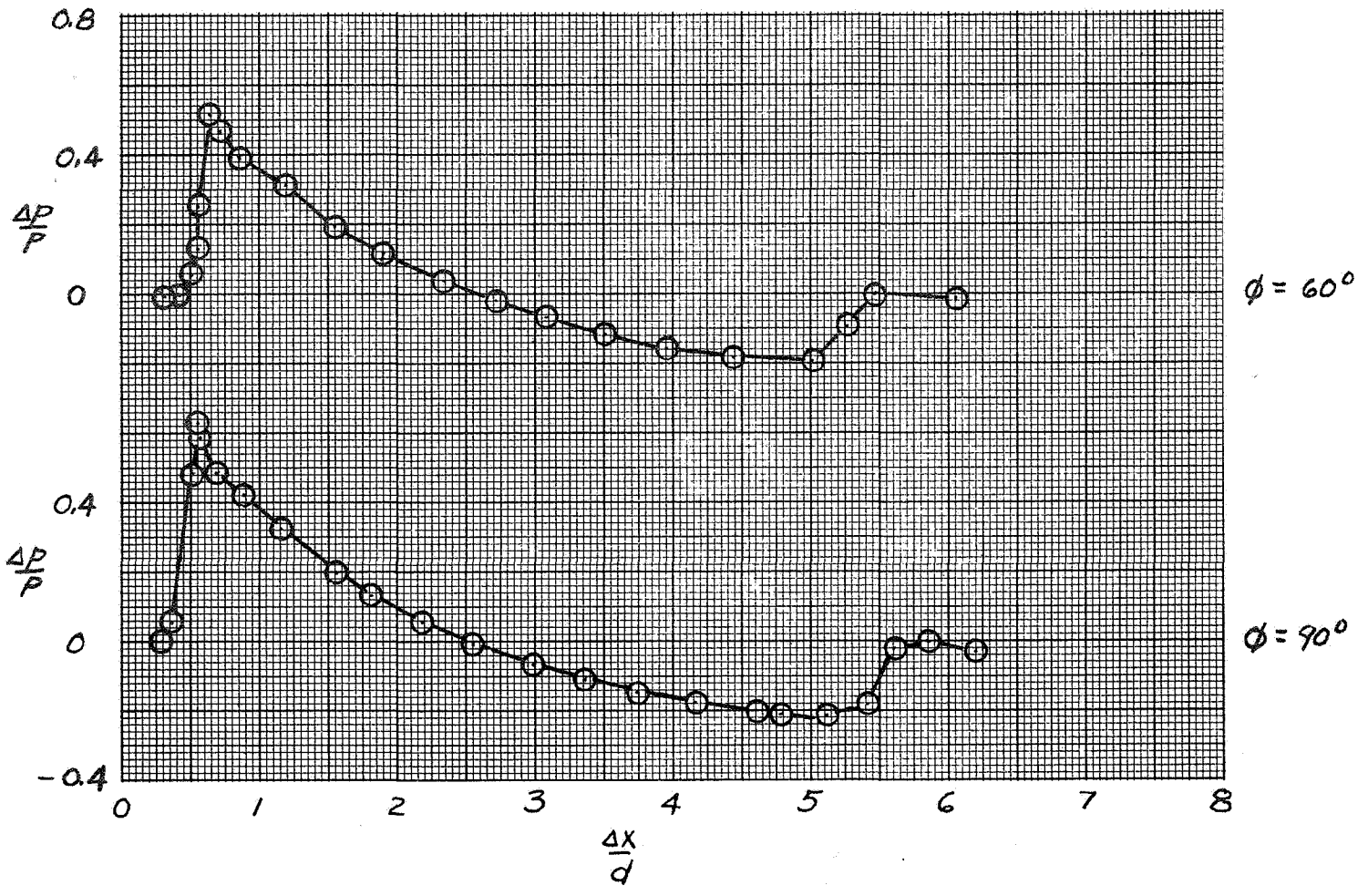

(b) $\phi = 60°, 90°$

Figure 6. - Continued

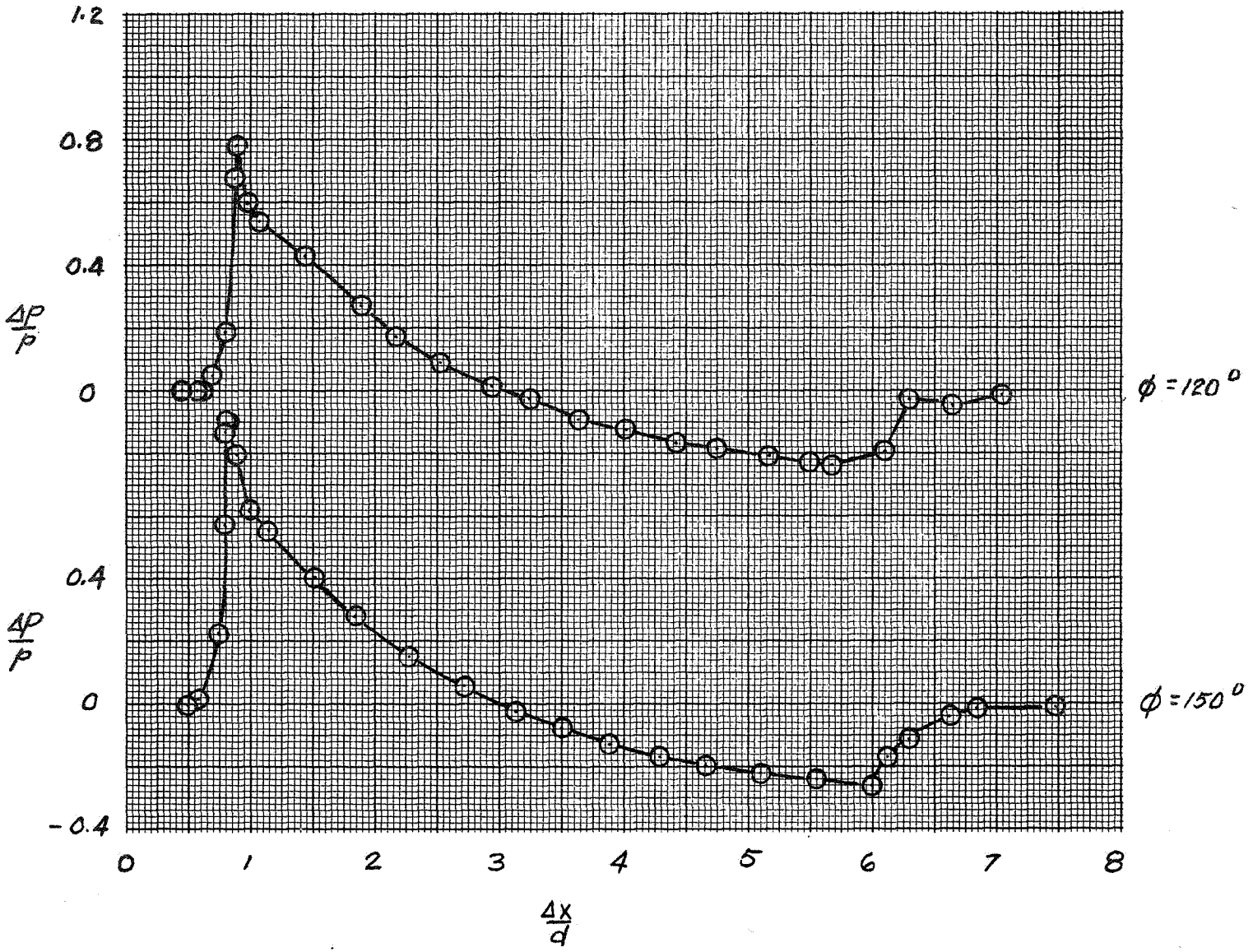

(c) $\phi = 120°, 150°$

Figure 6.- Continued

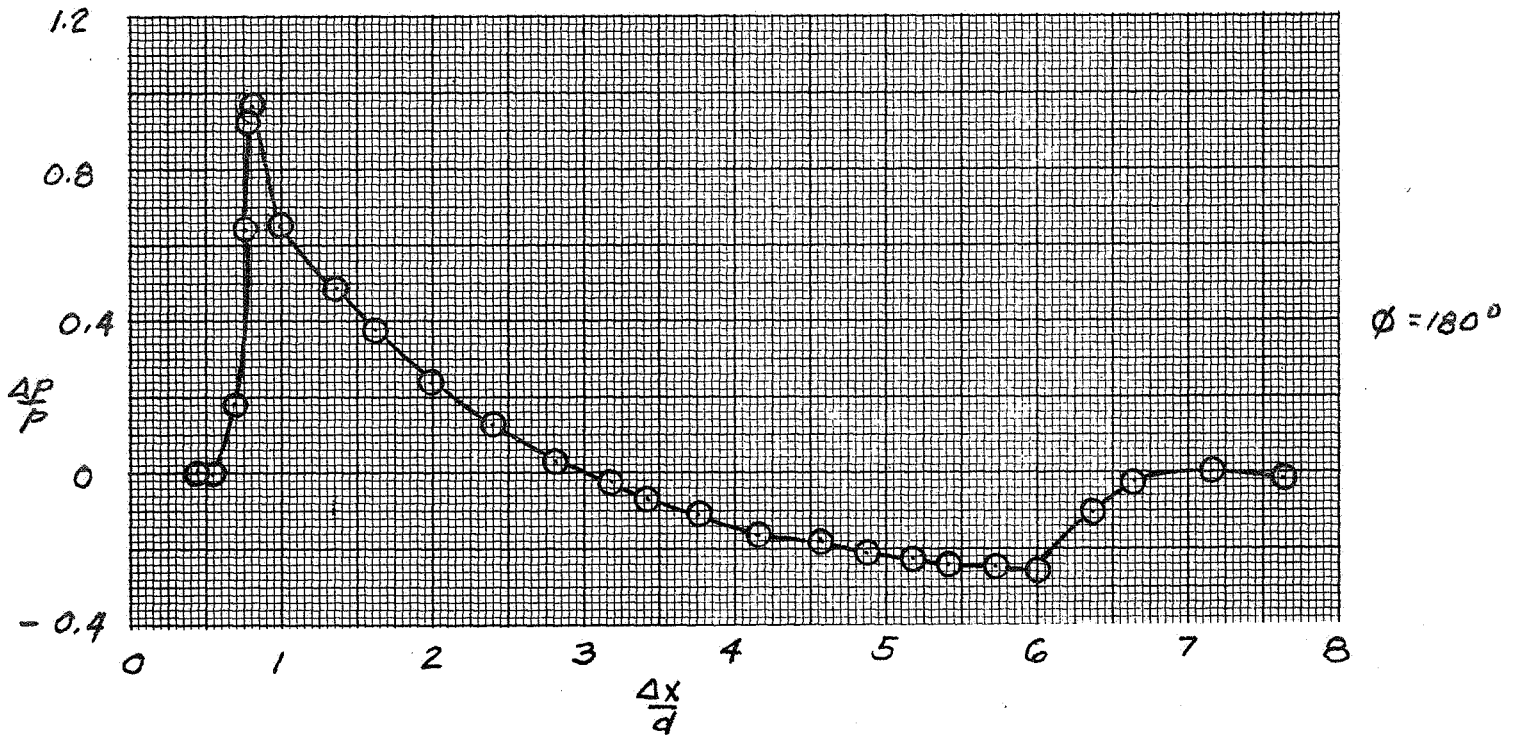

(d) $\phi = 180°$

Figure 6. - Concluded

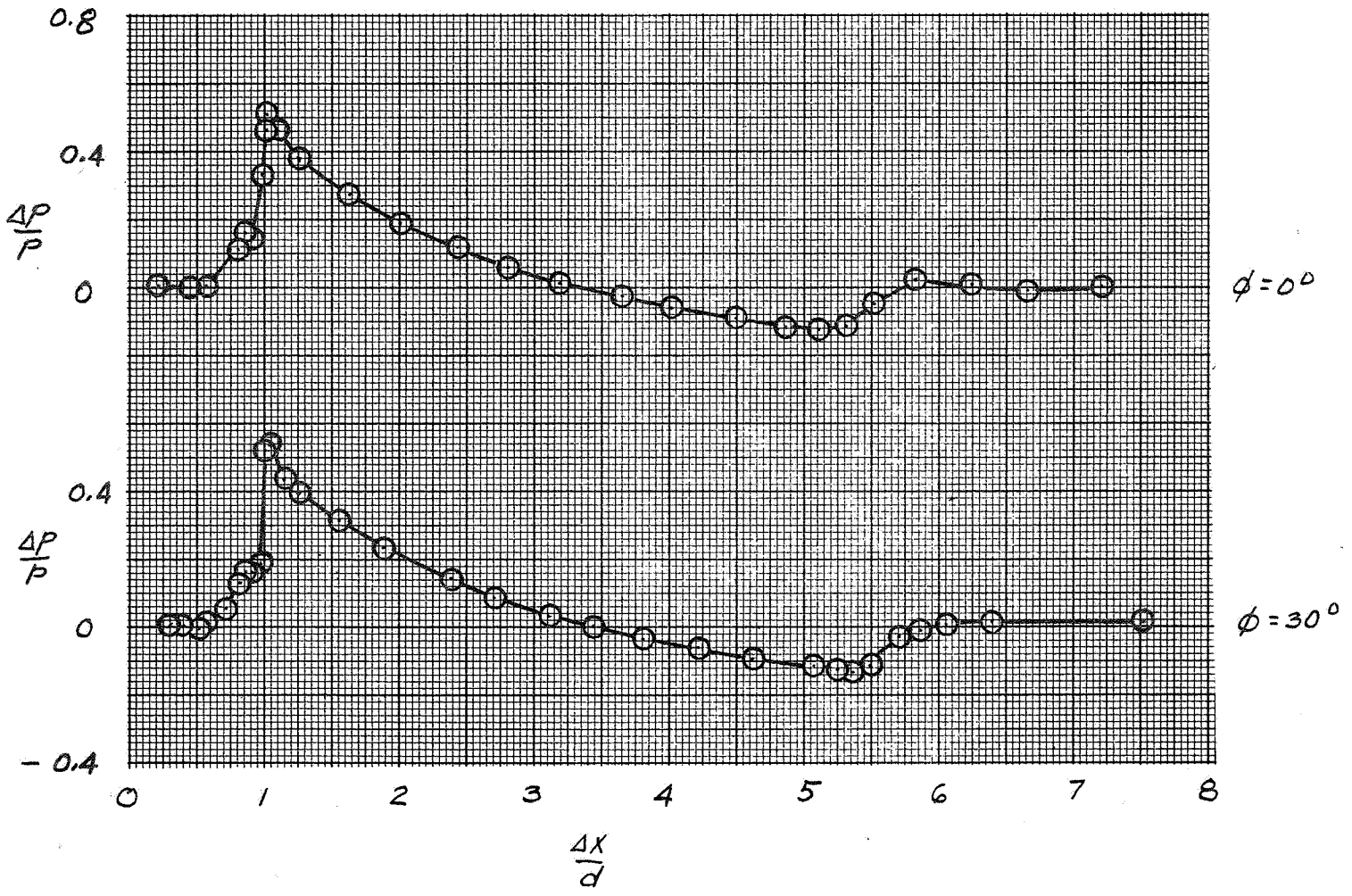

(a) $\phi = 0°, 30°$

Figure 7.- Pressure signatures, $M = 3.2$, $\alpha = 25°$, $h/d = 2.85$

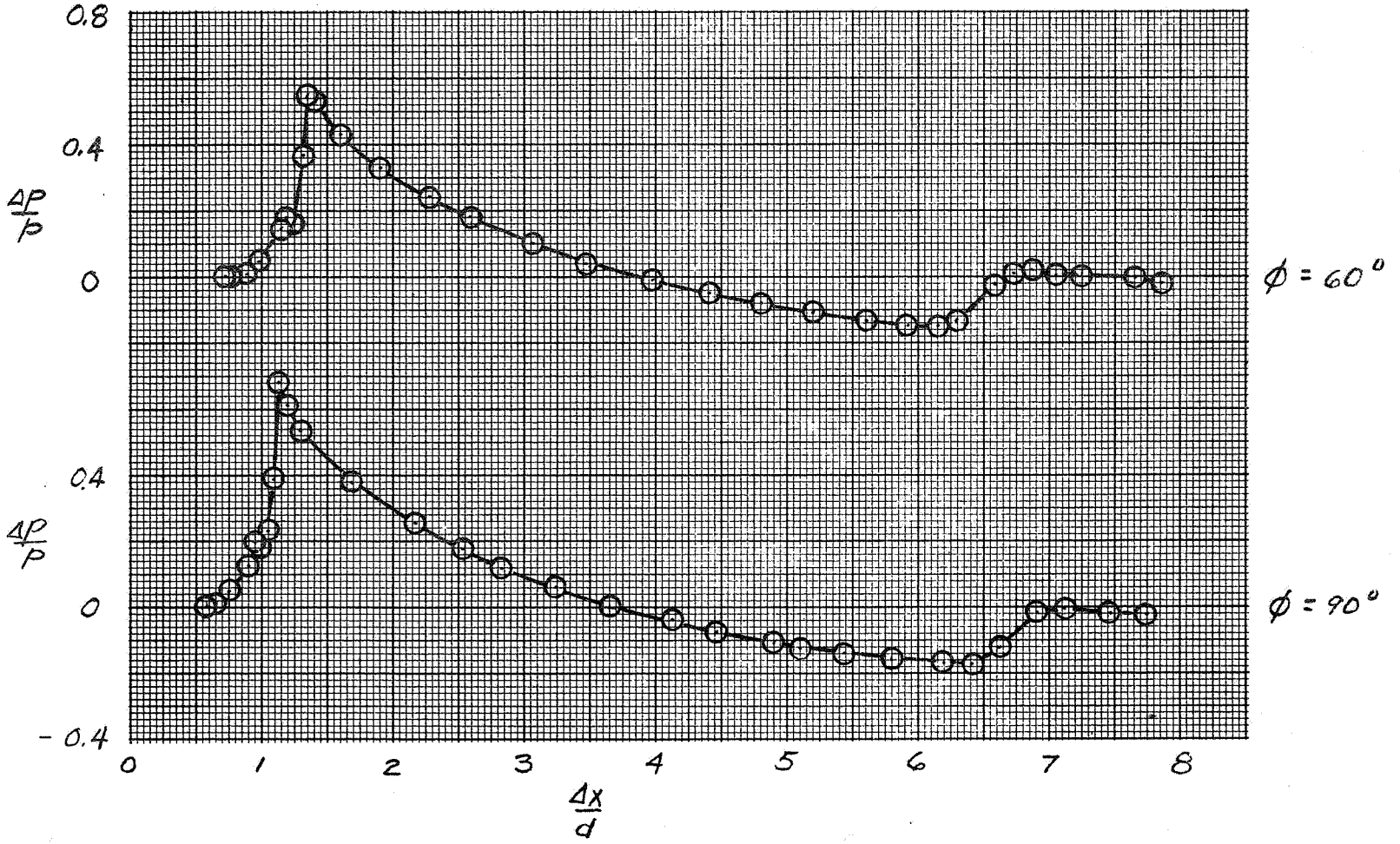

(b) $\phi = 60°, 90°$

Figure 7. - Continued

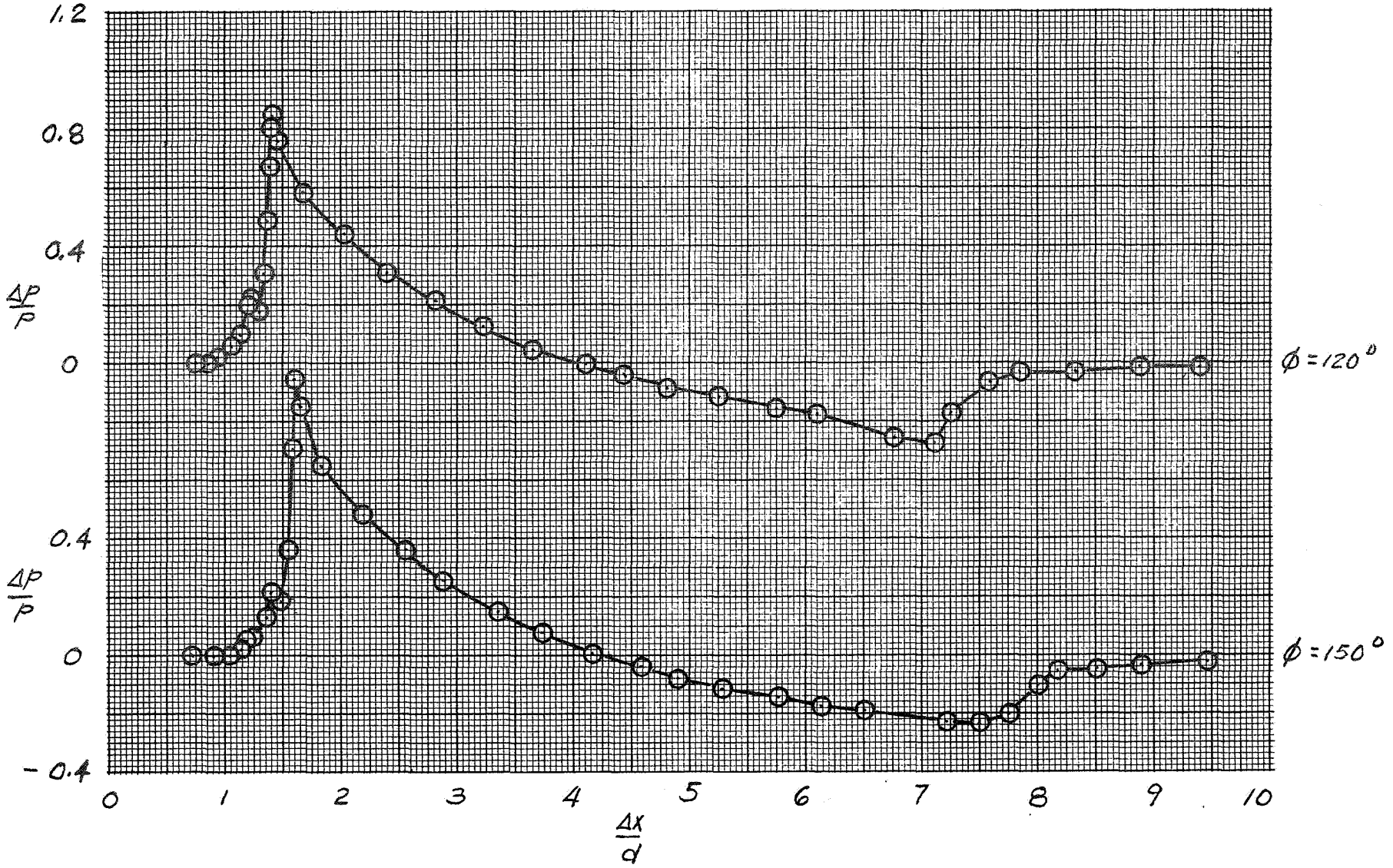

(c) $\phi = 120°, 150°$

Figure 7.- Continued

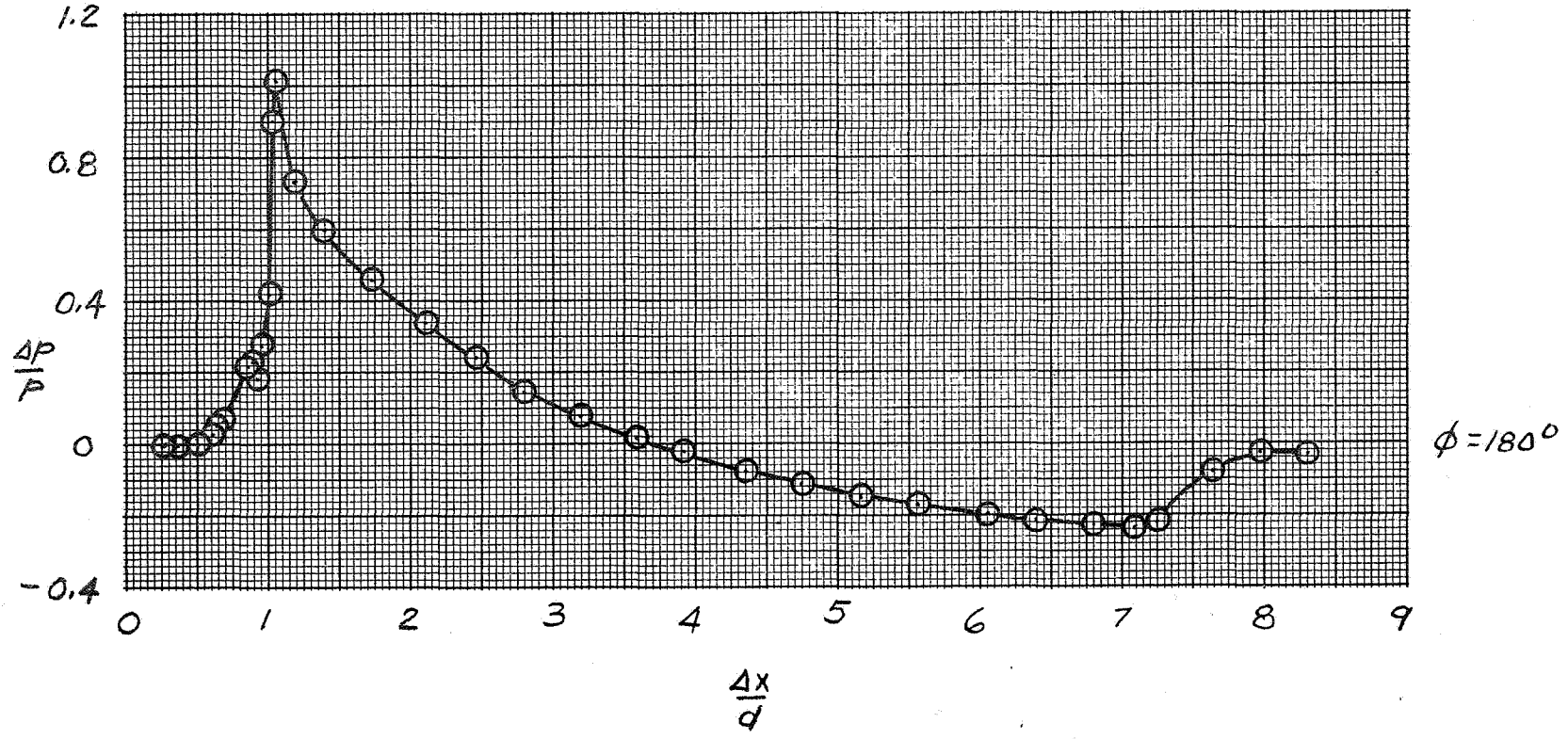

(d) $\phi = 180°$

Figure 7. - Concluded

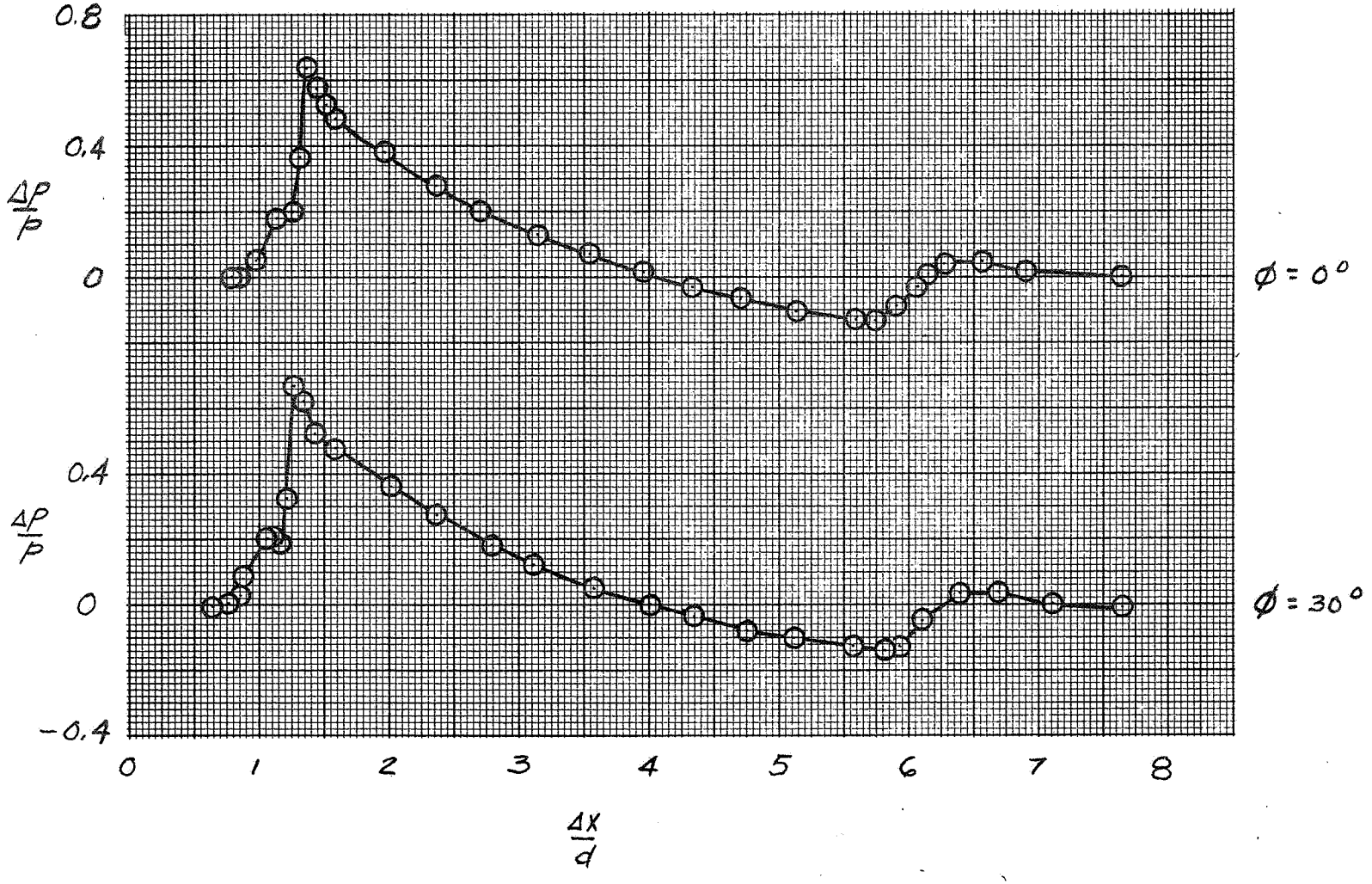

(a) $\phi = 0°, 30°$

Figure 8.- Pressure Signatures, $M = 3.98$, $\alpha = 25°$, $h/d = 2.85$

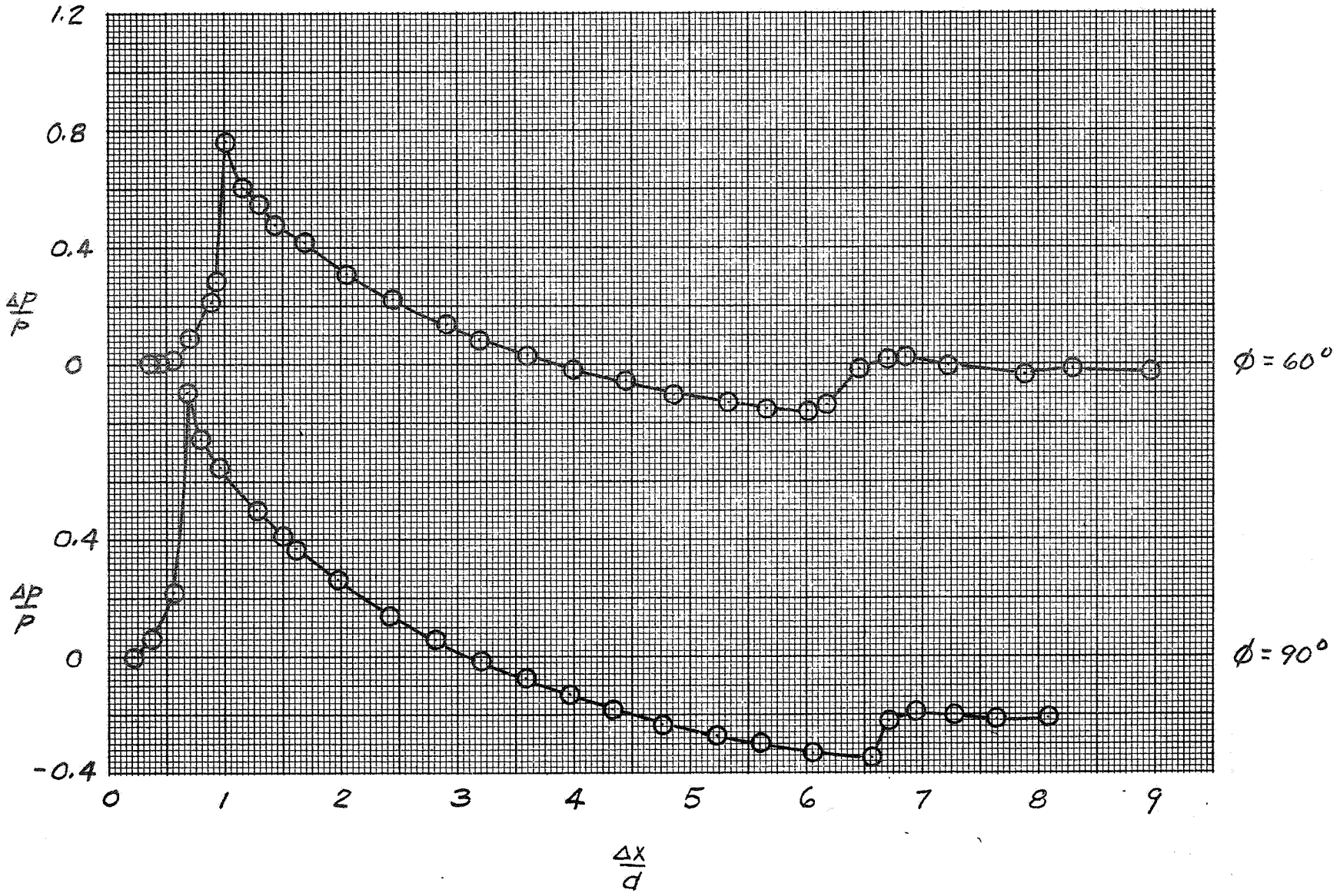

(b) $\phi = 60°; 90°$

Figure 8.- Continued

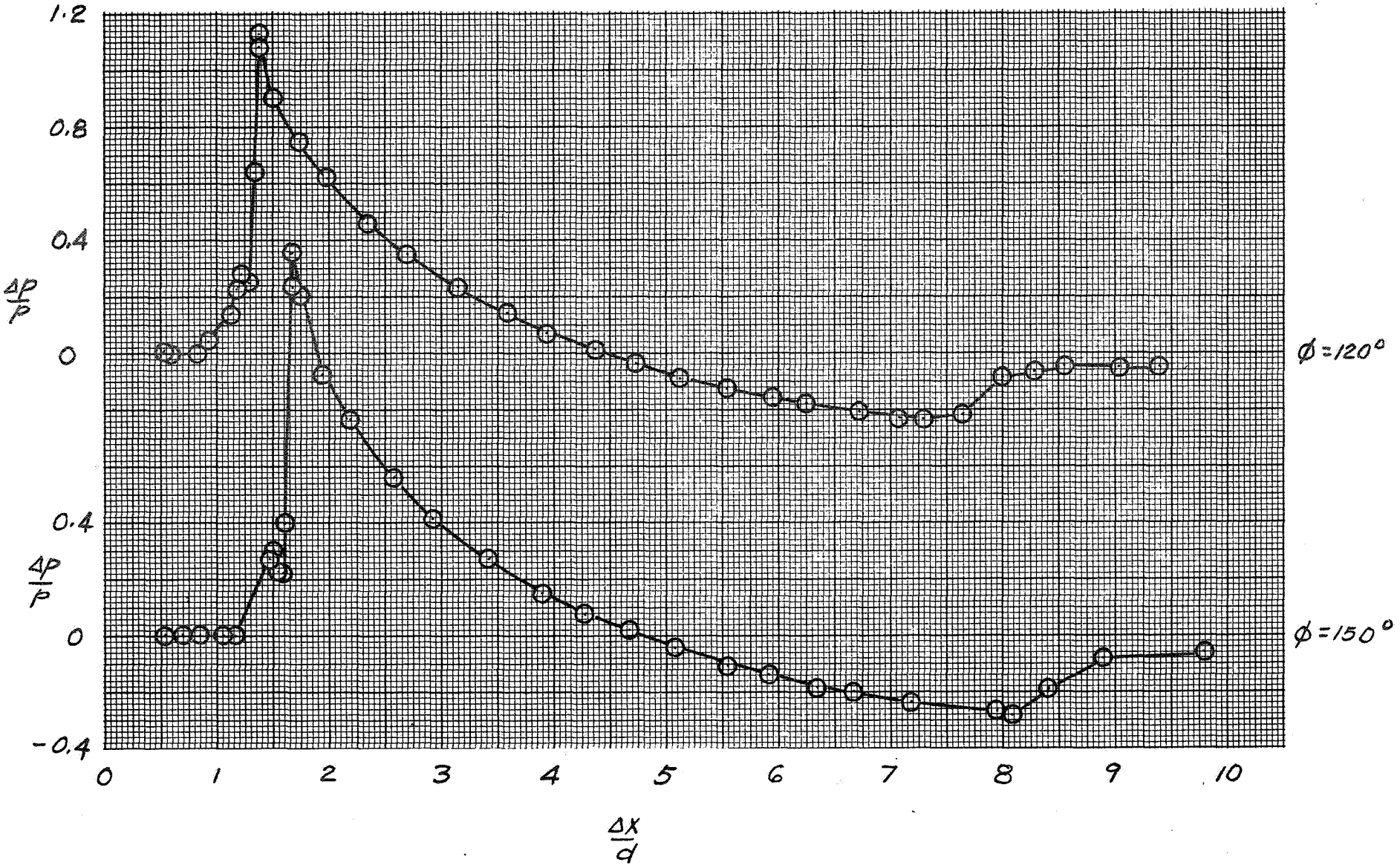

(c) $\phi = 120°, 150°$

Figure 8. - Continued

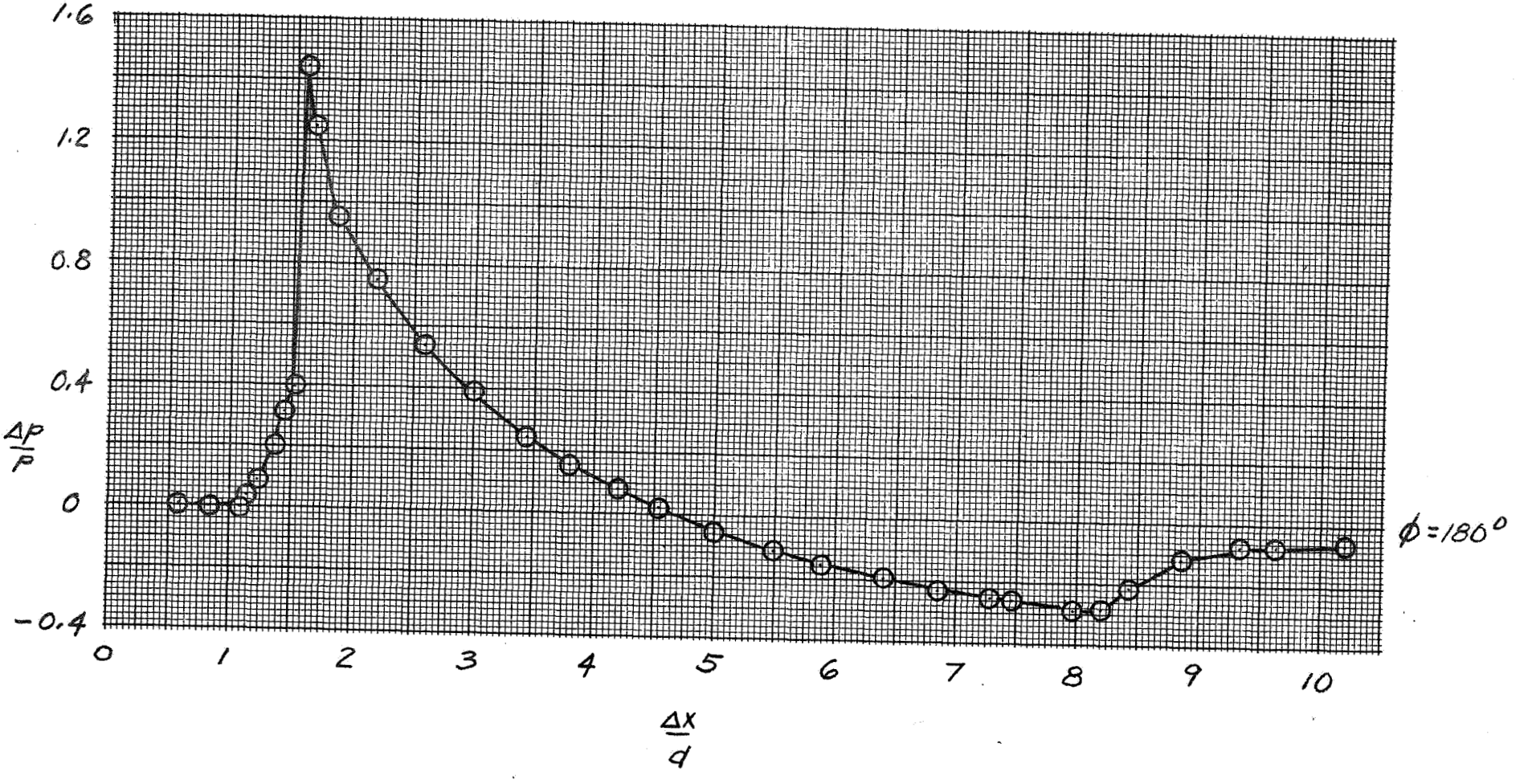

(d) $\phi = 180°$

Figure 8.- Concluded

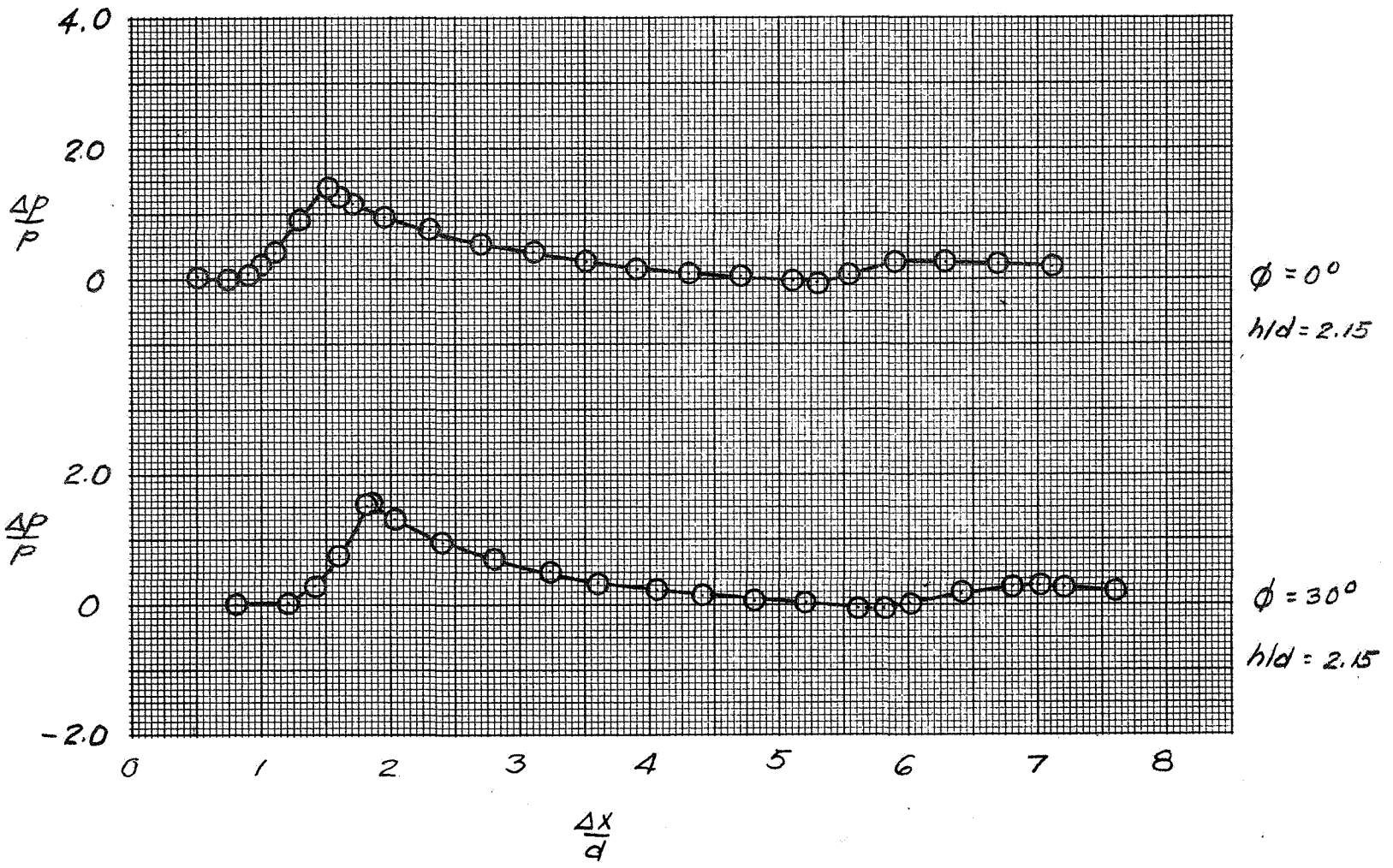

(a) $\phi = 0°, 30°$; $h/d = 2.15$

Figure 9. - Pressure Signatures, $M = 5.98$, $\alpha = 25°$

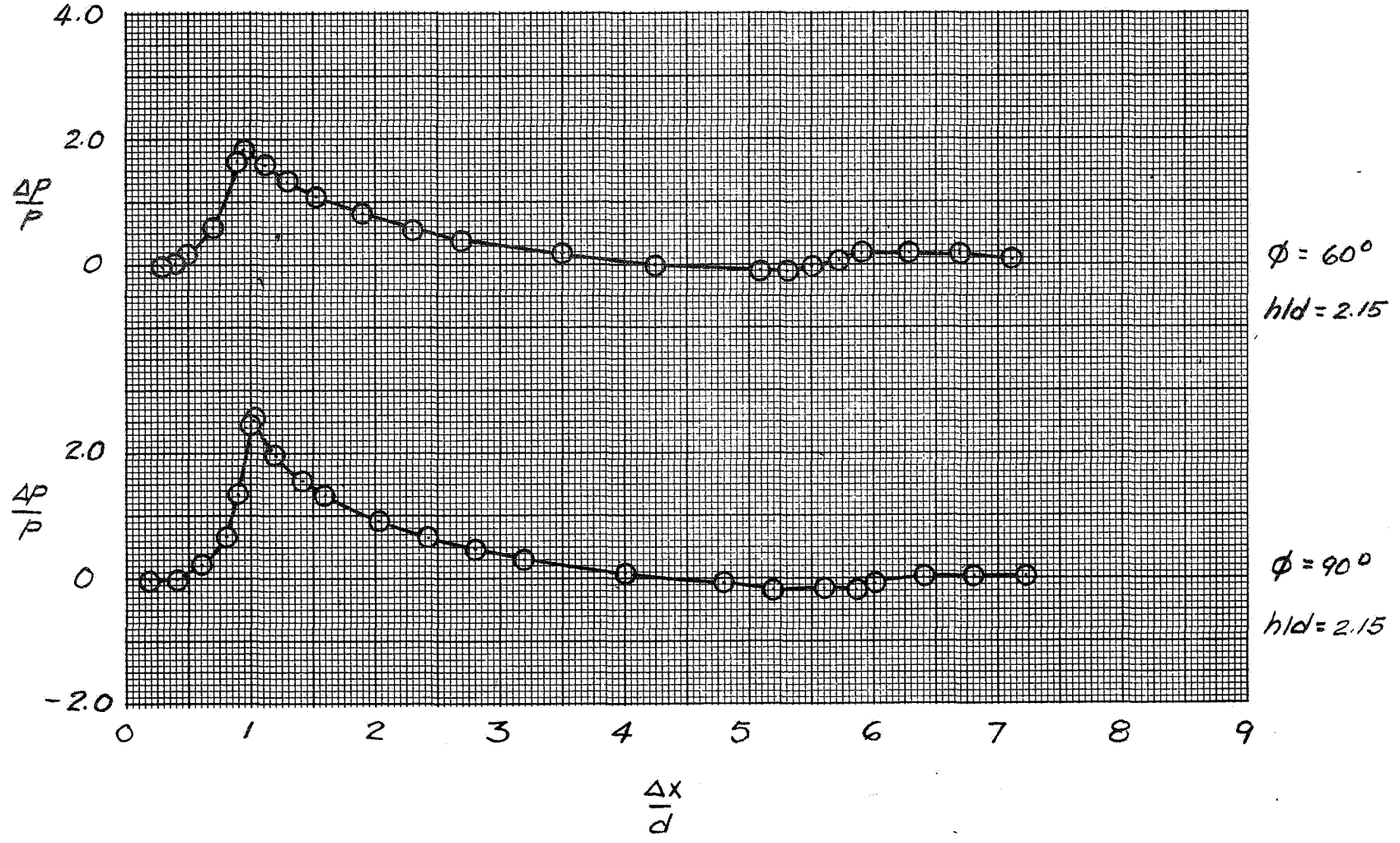

(b) $\phi = 60°, 90°; h/d = 2.15$

Figure 9. - Continued

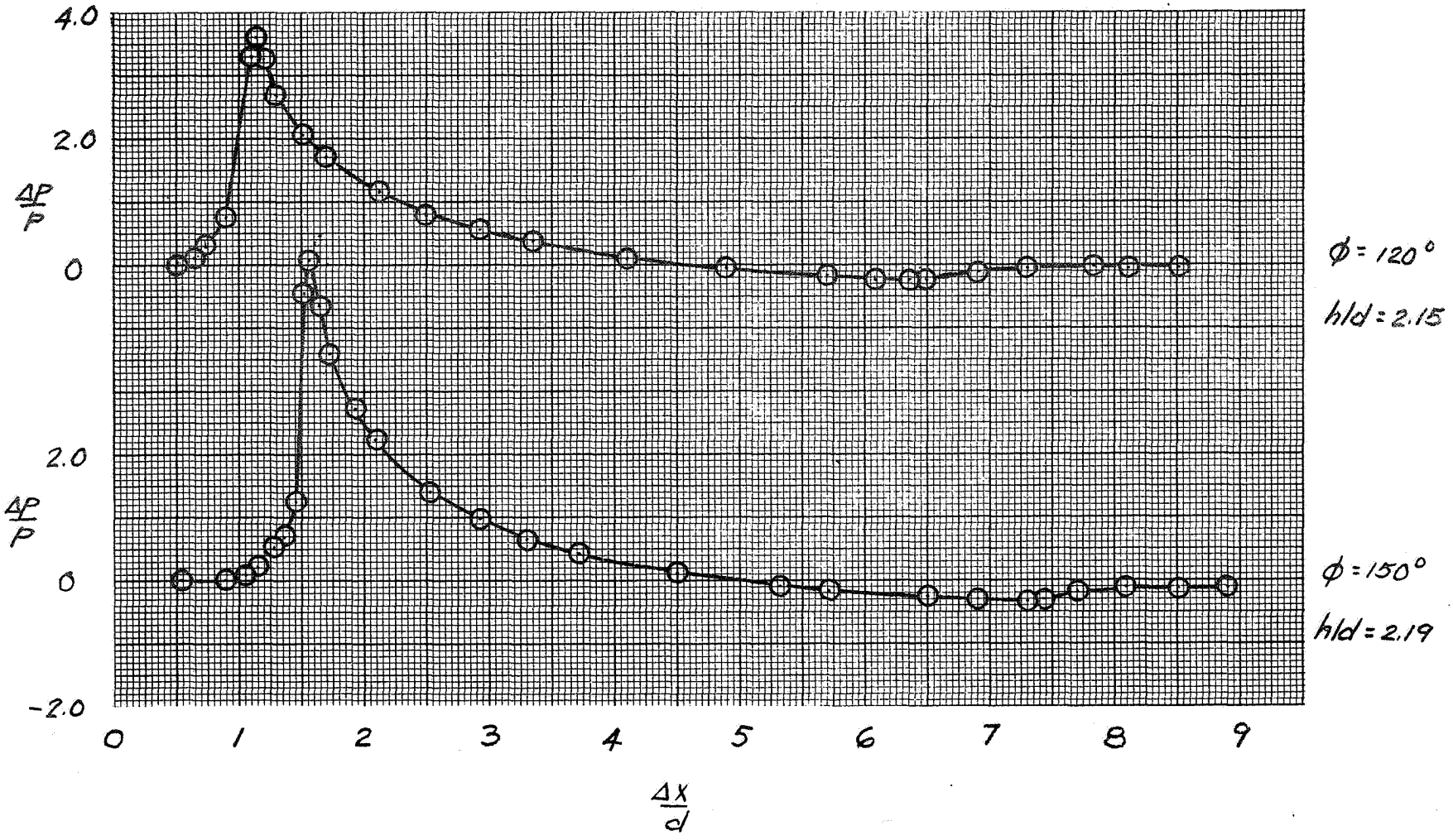

(c) $\phi = 120°$, $h/d = 2.15$; $\phi = 150°$, $h/d = 2.19$

Figure 9. - Continued

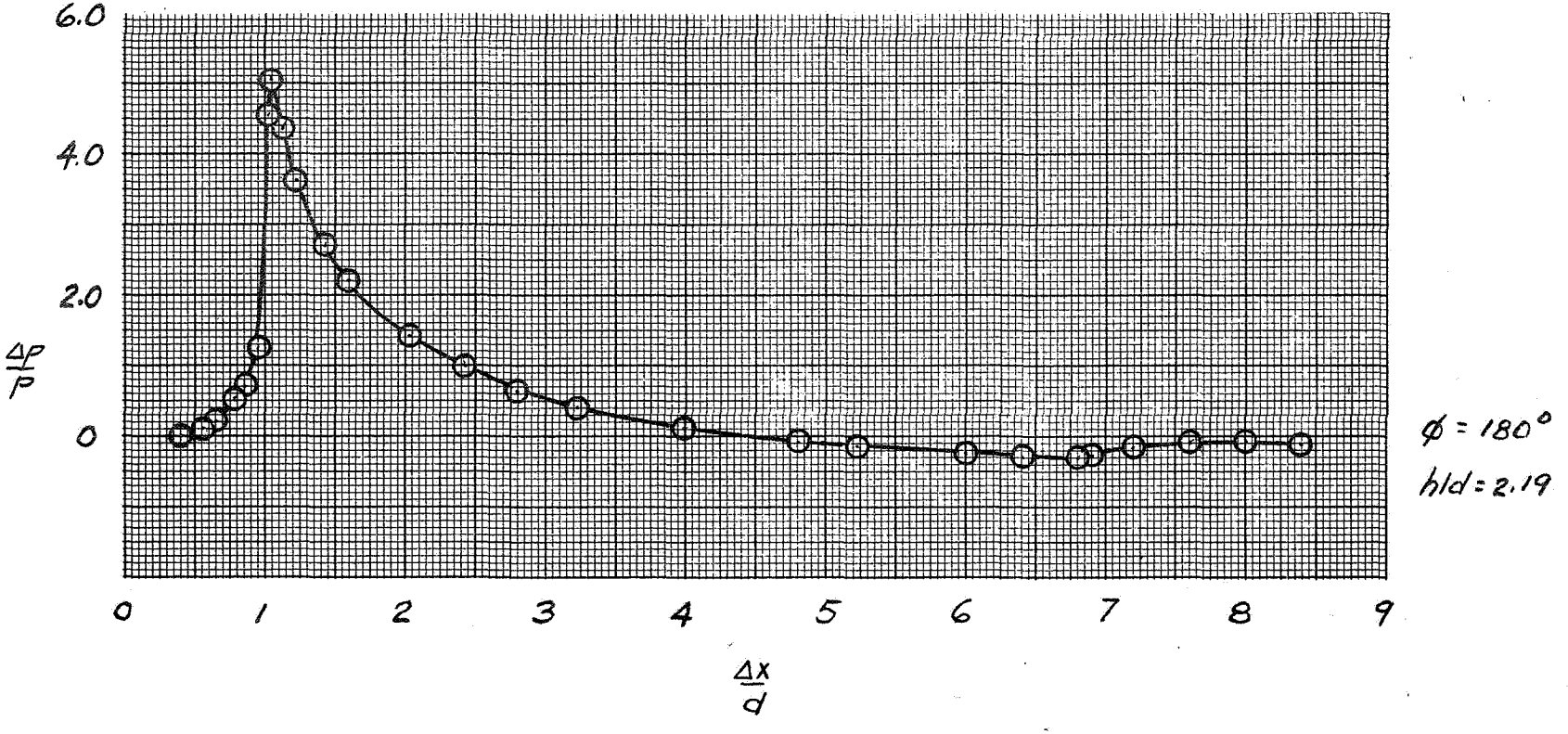

(d) $\phi = 180°$, $h/d = 2.19$

Figure 9. - Concluded

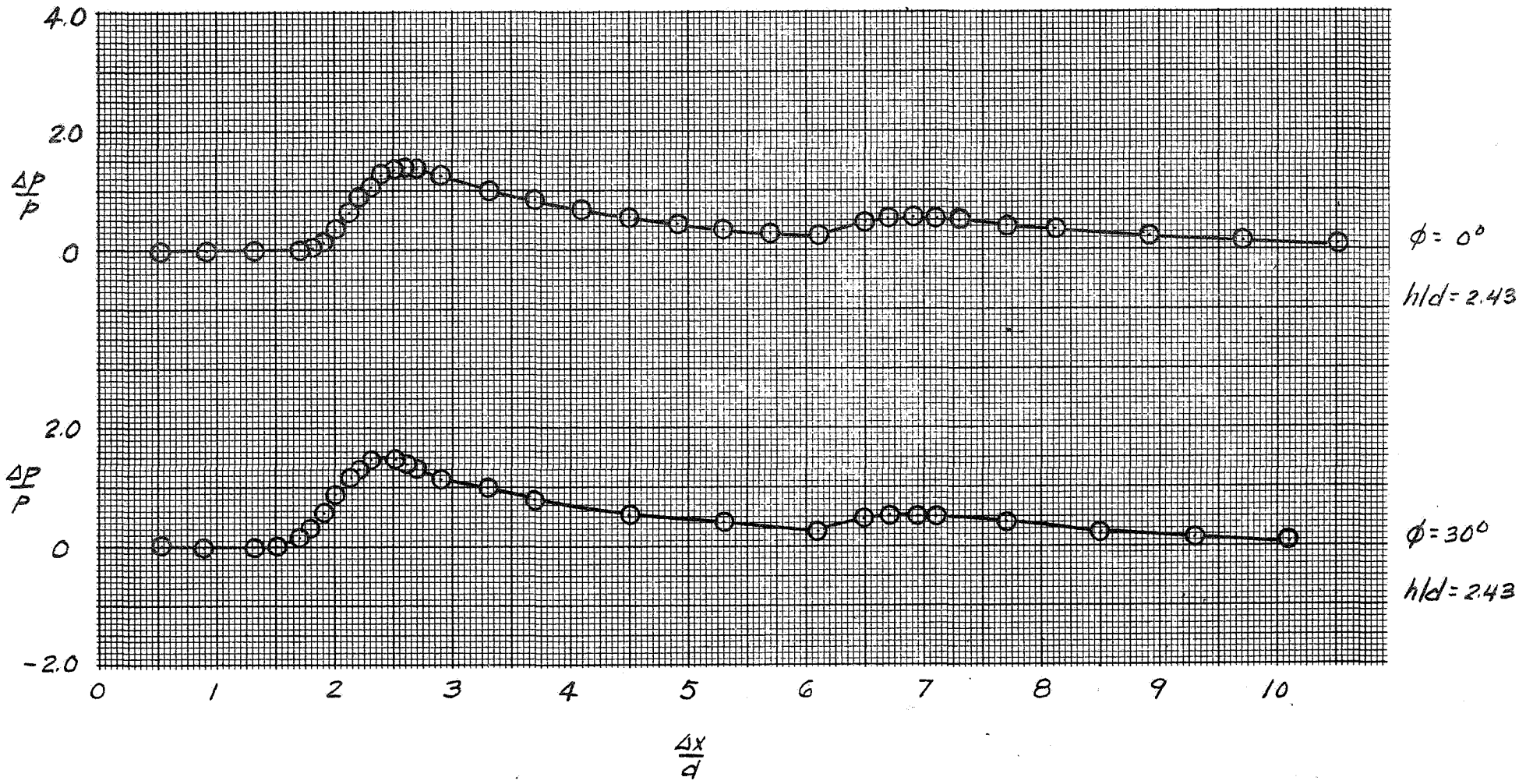

(a) $\phi = 0°, 30°$; $h/d = 2.43$

Figure 10.- Pressure Signatures, $M = 7.75$, $\alpha = 25°$

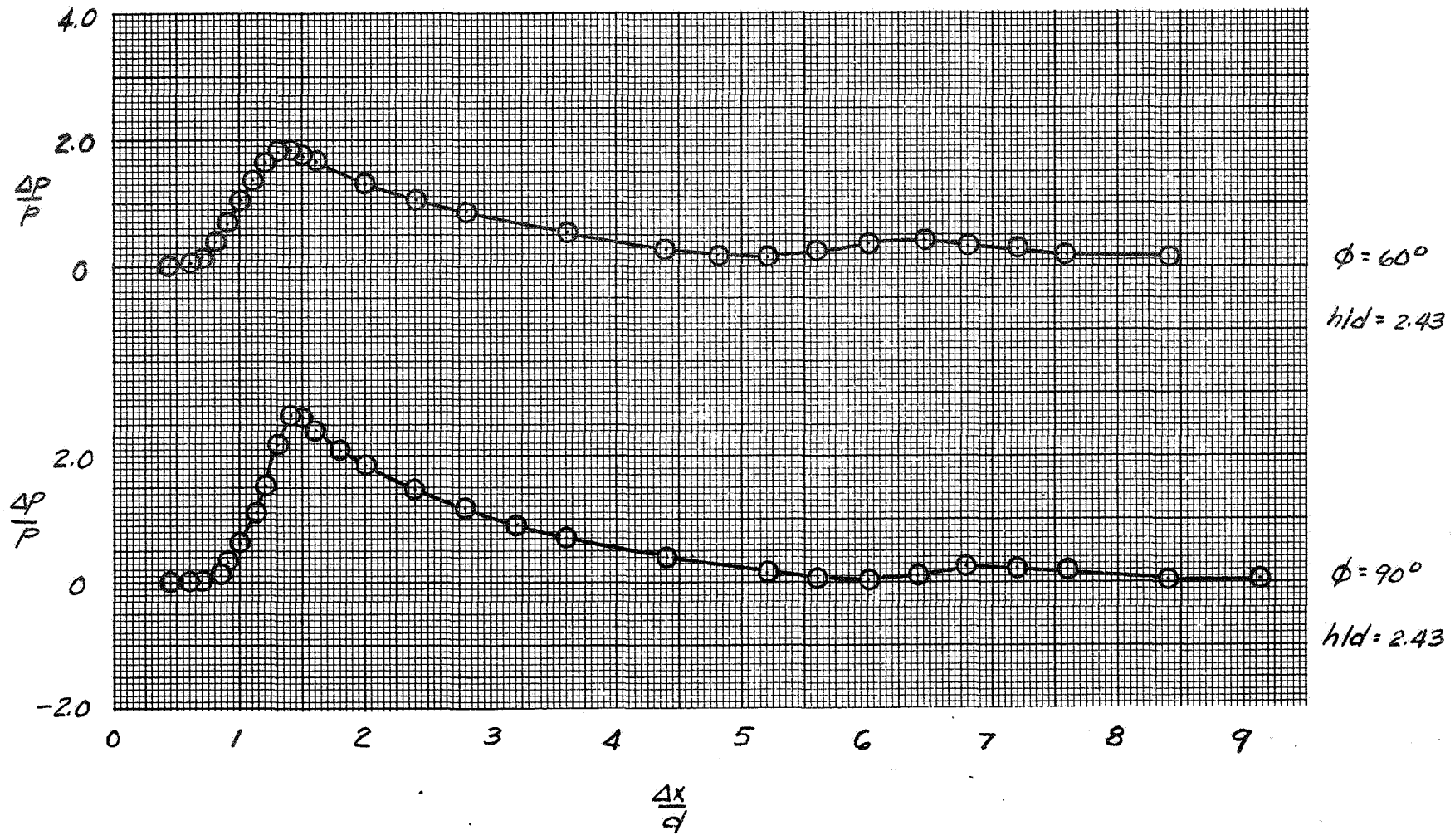

(b) $\phi = 60°, 90°$; $h/d = 2.43$

Figure 10.- Continued

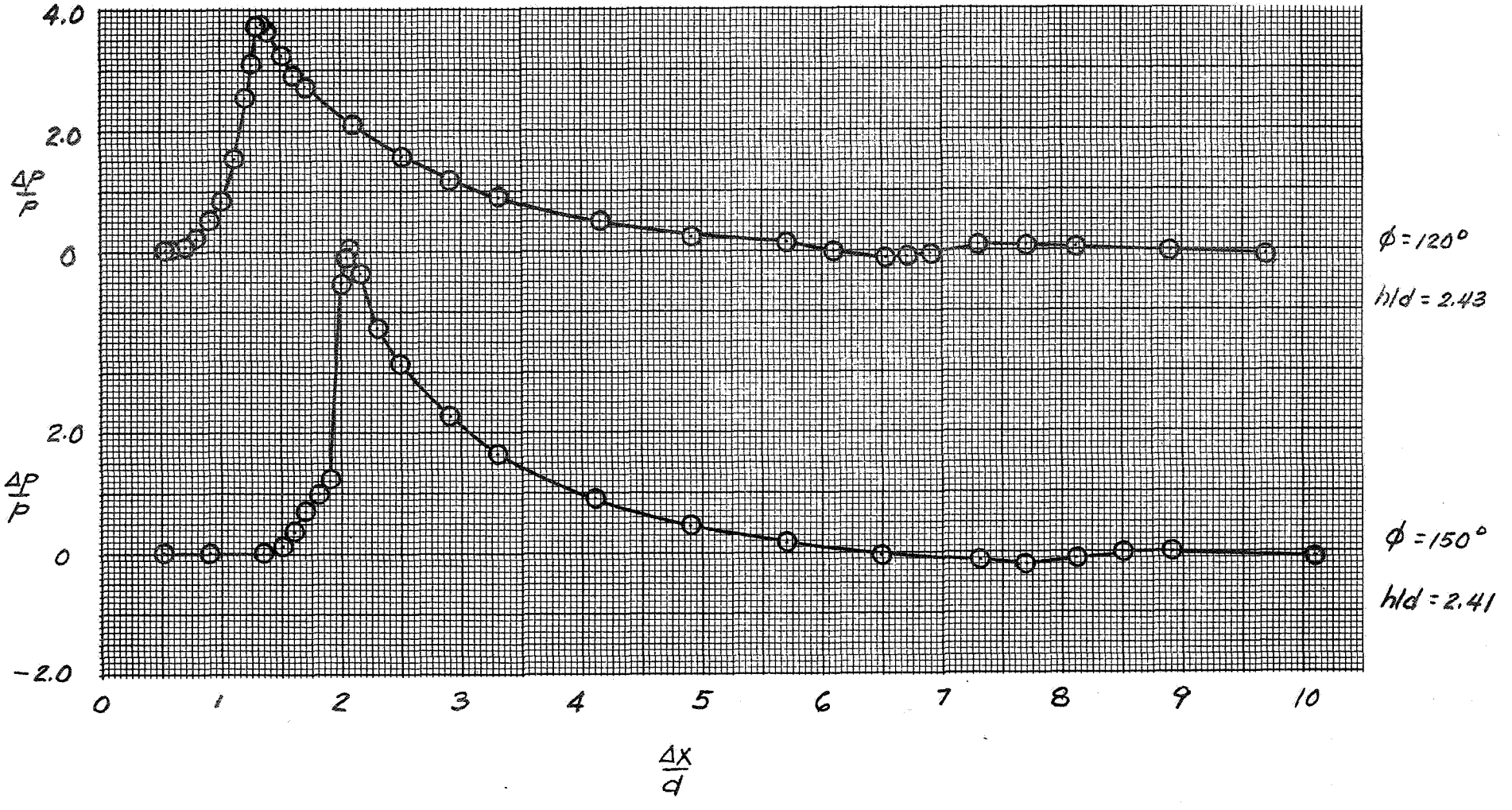

(c) $\phi = 120°$, $h/d = 2.43$; $\phi = 150°$, $h/d = 2.41$

Figure 10.- Continued

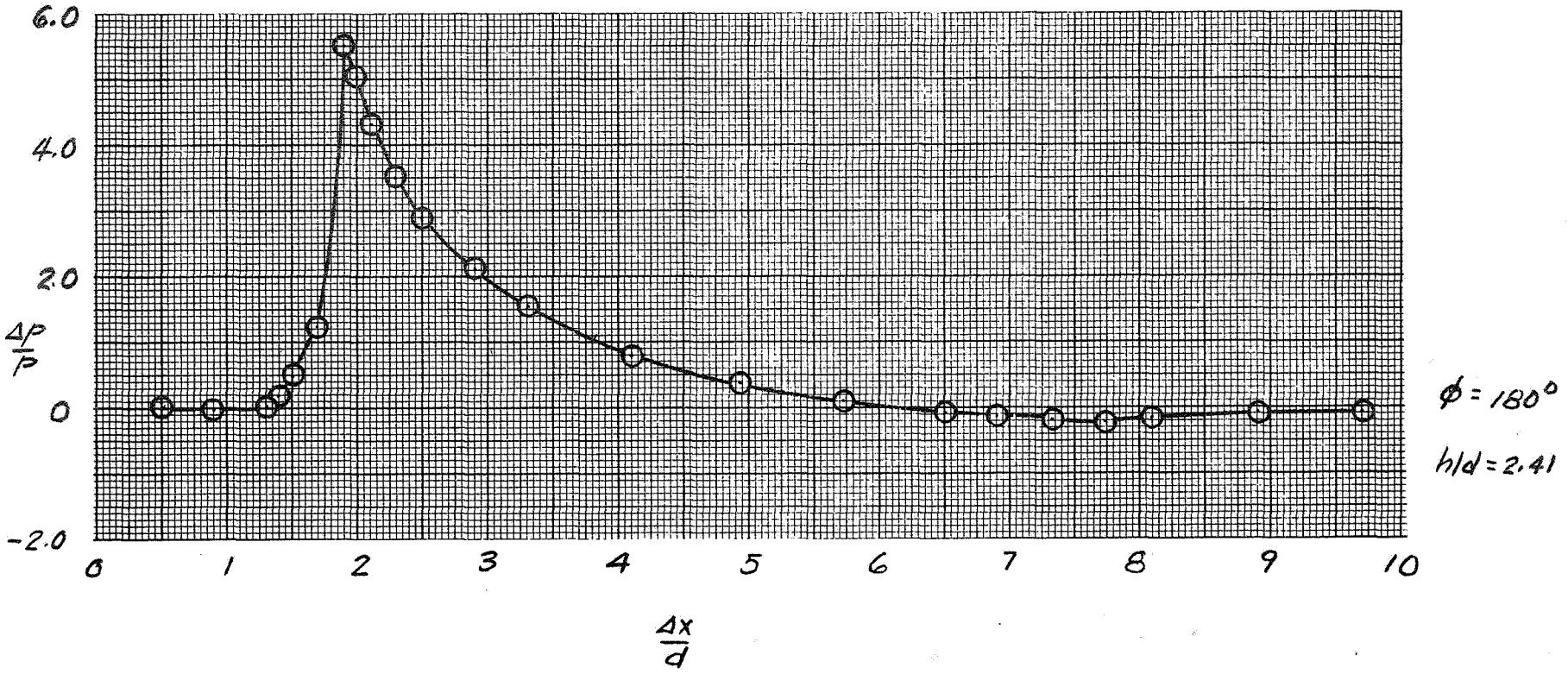

(d) $\phi = 180^\circ$, $h/d = 2.41$

Figure 10.- Concluded

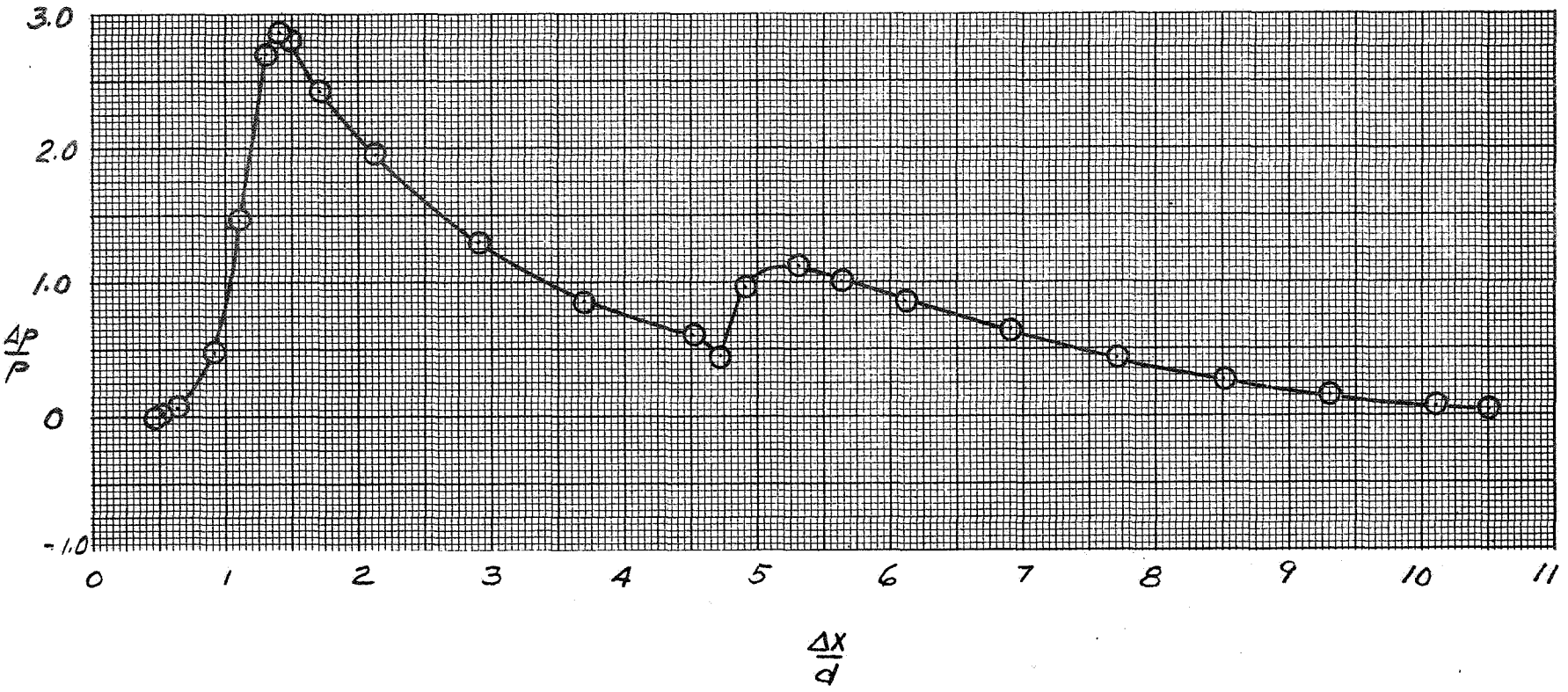

Figure 11. - Pressure signature, $M = 10.02$, $\alpha = 25°$, $h/d = 2.20$, $\phi = 0°$

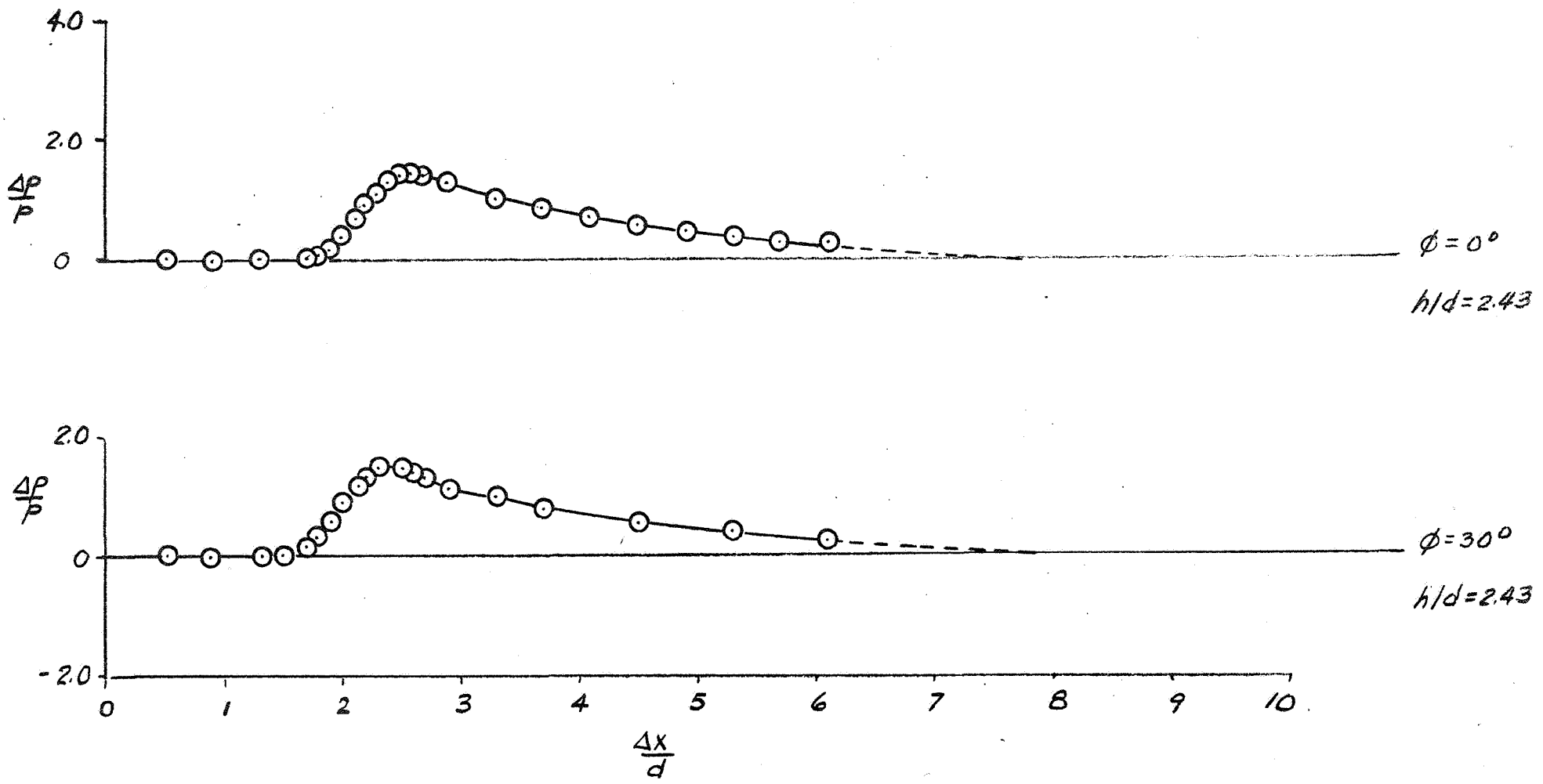

(a) M = 7.75

Figure 12.- Pressure signatures without sting interference.

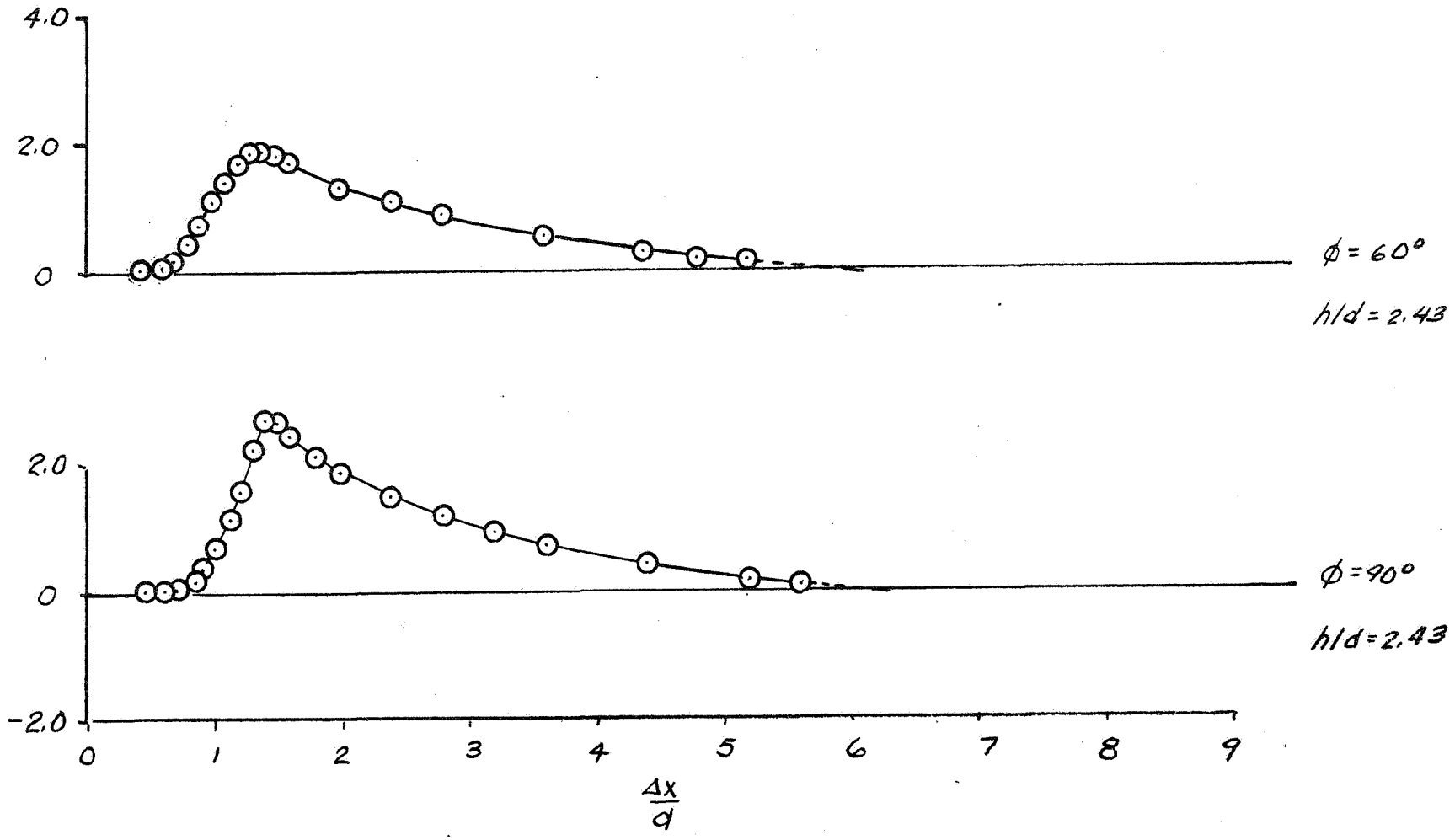

(b) $M = 7.75$

Figure 12.- Continued

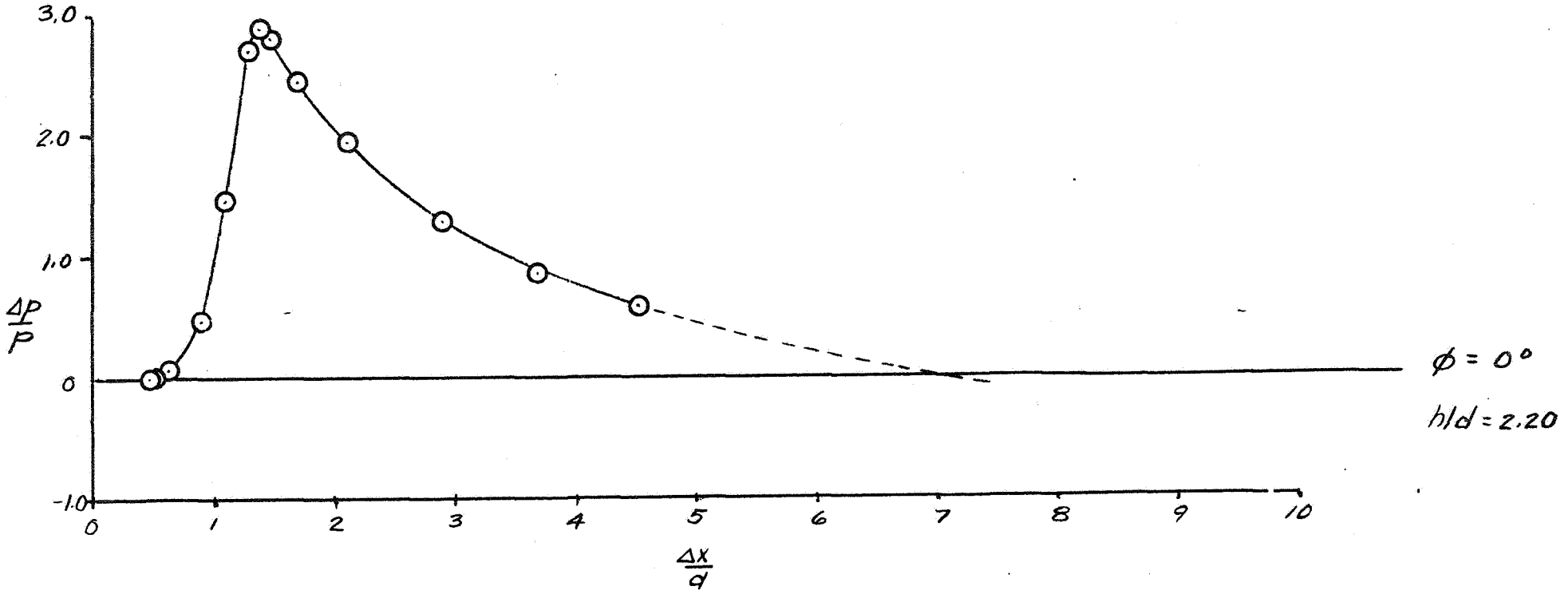

(c) $M = 10.02$

Figure 12.- Concluded